Using Nonlinear Normal Modes for Execution of Efficient Cyclic Motions in Soft Robots

Cosimo Della Santina[1], Dominic Lakatos[2,3], Antonio Bicchi[1,4], Alin Albu-Schaeffer[2,3]

***Abstract*—With the aim of getting closer to the performance of the animal muscleskeletal system, elastic elements are purposefully introduced in the mechanical structure of soft robots. Indeed, previous works have extensively shown that elasticity can endow robots with the ability of performing tasks with increased efficiency, peak performances, and mechanical robustness. However, despite the many achievements, a general theory of efficient motions in soft robots is still lacking. Most of the literature focuses on specific examples, or imposes a prescribed behavior through dynamic cancellations, thus defeating the purpose of introducing elasticity in the first place.**

This paper aims at making a step towards establishing such a general framework. To this end, we leverage on the theory of oscillations in nonlinear dynamical systems, and we take inspiration from state of the art theories about how the human central nervous system manages the muscleskeletal system. We propose to generate regular and efficient motions in soft robots by stabilizing sub-manifolds of the state space on which the system would naturally evolve. We select these sub-manifolds as the nonlinear continuation of linear eigenspaces, called nonlinear normal modes. In such a way, efficient oscillatory behaviors can be excited. We show the effectiveness of the methods in simulations on an elastic inverted pendulum, and experimentally on a segmented elastic leg.

***Index Terms*—Soft Robotics, Compliantly Actuated Robots, Robot Control, Nonlinear Normal Modes, Human Inspired Control.**

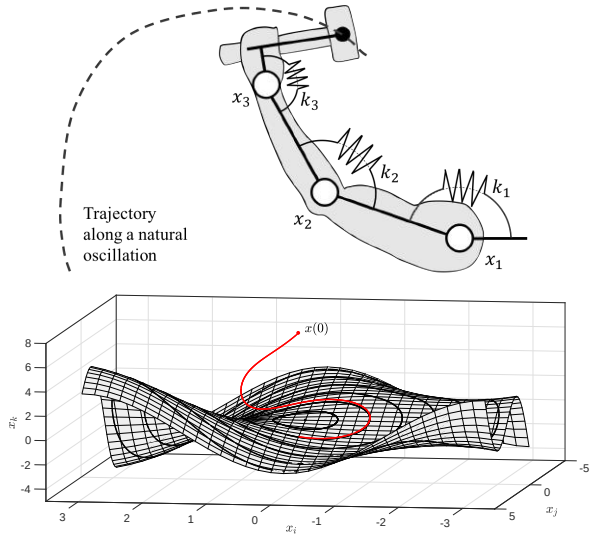

Figure 1. Exploiting the muscle-skeletal dynamics, humans are able to generate efficient multi-DoF natural oscillations by stabilizing manifolds of reduced dimensionality, called UCM. Similarly, we propose to generate efficient cyclic motions in soft robots by individuating in invariant modal manifolds an artificial counterpart of the natural UCM, which we then make attractive by control.

I. Introduction

Actuation in living beings shows characteristics very different from the classic rigid robotic structures. Tendon and muscles elasticity, rather than being an impediment, enables animals to robustly interact with the external world and to efficiently perform dynamic and oscillatory tasks [1]. Inspired from the natural actuation, in soft robots elastic elements are purposefully introduced in the mechanical structure. Two main branches exist in soft robotic research according to their main source of inspiration. The first one involves robots made by continuously flexible materials. In analogy to the animal invertebrate body, the compliance is here distributed in the whole structure [2]. Notable examples are [3], [4], [5]. The other branch is instead inspired by the vertebrate muscleskeletal system. Here the compliance is mostly concentrated in the joints [6]. Such robots are typically referred as articulated soft robots or compliantly actuated robots. Examples are [7], [8], [9], [10], [11].

This work is supported by .

[1]Research Center "Enrico Piaggio", University of Pisa, Largo Lucio Lazzarino 1, 56126 Pisa, Italy

[2] Institute of Robotics and Mechatronics, German Aerospace Center (DLR), Oberpfaffenhofen 82234, Germany

[3]Department of Advanced Robotics, Istituto Italiano di Tecnologia, via Morego, 30, 16163 Genova, Italy

cosimodellasantina@gmail.com

Together with the new possibilities, soft robotics comes with the new challenge of developing control strategies being able to properly exploit the intelligence embedded in the robot mechanics [12], [13]. Several works exist in literature, where analytical optimal control is used to derive strategies fully exploiting the dynamics of soft robots, e.g. in terms of adaptability and safety [14], maximization of peak performances [15], efficient execution of cyclic motions [16]. However, while very effective in generating meaningful strategies, analytical optimal control is limited to low dimensional systems and specific tasks. Thus, to reach a full exploitation of the intrinsic soft robot dynamics, the investigation of more general paradigms is crucial.

In this work we specifically target the problem of generating regular oscillatory behaviors in soft robots with multiple degrees of freedom (see Fig. 1). Classical techniques of trajectory tracking can be used to reach this goal, such as feedback linearization [17], backstepping [18], adaptive control [19], just to cite a few. However, as discussed in [20], these approaches deeply change the plant inherent behavior. Instead of exploiting the intelligence embodied by design, they replace the natural dynamics with a different desired model, defeating the main purpose of introducing physical compliance. With the aim of overcoming this limitation novel approaches specifically designed for soft robotic systems were proposed. In [21] the model of an elastically actuated segmented leg is

matched to the SLIP one. In [22] joints dynamics is decoupled by control, canceling Coriolis, centrifugal and gravitational effects, in combination with energy regulation. In [23] virtual holonomic constraints are imposed, again in combination with energy regulation. However, these techniques still envisage a certain level of dynamics cancellation, which results only in a partial exploitation of the intrinsic system dynamics.

Looking instead at the natural world, humans are able to intuitively execute complex oscillatory movements, exploiting the muscleskeletal dynamics [24] despite the vast abundance of the body degrees of freedom. This ability was pinpointed for the first time by Nicolaj Bernstein [25], in the so-called *motor equivalence problem*. According to more recent neuro-scientific theories [26], [27], the central nervous system is able to implement such a behavior by stabilizing a set of *variables of interest*, while leaving the remaining degrees of freedom to evolve naturally. Regulating these variables implicitly identify a manifold, the so-called UnControlled Manifold, or UCM. The neural mechanism deputed to UCM stabilization is referred as *synergy* [28].

Inspired by these neuro-scientific evidences, we propose to exploit the soft robot's embodied intelligence by stabilizing manifolds of reduced dimensionality on which the robot can naturally evolve. The evolution is natural in the sense that it is a direct expression of the autonomous dynamics of the physical system. The theory that studies these manifolds in dynamical system field is the so-called *modal analysis*, which is a classical result in linear systems theory. Nonlinear extensions of this concept are a more recent development, taking the name of Nonlinear Normal Modes [29]. To the best of authors knowledge, their application to robotic systems analysis and control is considered here for the first time, while the application of so-called similar normal modes were investigated in [30] (see Sec. III for more details).

In this work we consider the control of soft robots that can be modeled with a finite set of ordinary differential equations. This of course includes articulated soft robots, and we will focus mostly on them for the sake of tractability. However, in the past few years, several works [31], [32], [33], [34] demonstrated that continuously deformable robots can be described at any given level of accuracy through a finite dimensional discretization. So the proposed results are to be considered generally applicable also to continuous and hybrid kinds [35].

The work is organized as follow. In Sec. II the control strategy is introduced and discussed in the linear case. In Sec. III we survey the literature related to the non linear extensions of linear modal analysis. In Sec. IV the nonlinear case is faced, and a control algorithm assuring the modal manifold attractiveness is proposed. The problem of exciting a specific orbit on the manifold is also discussed. In Sec. V we apply the proposed strategy to the control of a spring loaded inverted pendulum. The modal analysis is discussed, and simulations are provided. Finally an experimental validation of the robustness of the control architecture is proposed in Sec. VI. Conclusions are drawn in Sec. VII.

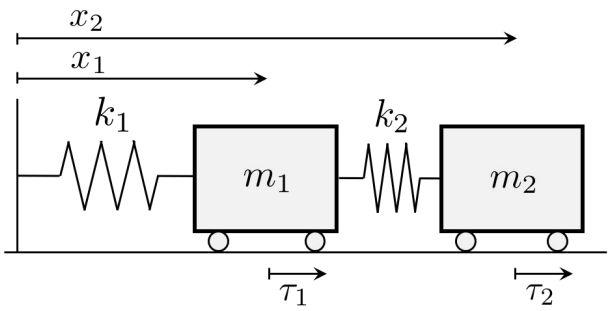

Figure 2. A simple example of soft robotic system with linear dynamics. m_1 and m_2 are the masses of the two bodies, while x_1 and x_2 are their positions. k_1 is the stiffness of the spring connecting the first body to ground, while k_2 is the stiffness of the spring connecting the two bodies together. Two forces τ_1 and τ_2 can be independently exerted on the masses.

II. Linear Case

We consider as simplest prototype of soft robotic systems with n degrees of freedom (DoFs hereinafter), the following generic linear mechanical system

$$M\ddot{x} = -Kx + \tau\,, \tag{1}$$

where $x \in \mathbb{R}^n$ are the system's configuration coordinates. $K \in \mathbb{R}^{n\times n}$ such that $K = K^T \succ 0$ is the stiffness matrix. $M \in \mathbb{R}^{n\times n}$ such that $M = M^T \succ 0$ is the inertia matrix. $\tau \in \mathbb{R}^n$ are the generalized forces. For the sake of brevity, we consider the system to be conservative. However all the arguments that follow are easily generalizable to the dissipative case.

The natural oscillations of a linear mechanical system are well studied in the classic linear system theory. In this case unforced evolutions are always a linear combination of a finite set of normal modes, in number less or equal to the DoFs. The modal evolutions can be evaluated as complex exponential of the system's eigenvalues. Each mode evolves in its own eigenspace spanned by the generalized eigenvectors associated to the mode. The projection of an eigenspace in the configuration space indicates the directions of oscillation. In non dissipative systems these directions can be directly evaluated through spectral decomposition of the matrix $M^{-1}K$. For a complete description of modal analysis and resonance in linear systems please refer to [36].

Thanks to these well known properties, designing control strategies exploiting the dynamics of a linear system to generate natural oscillatory behaviors is a relatively simple task. Lets examine the problem of stabilizing the system in one of its eigenspaces. We consider without loss of generality the eigenspace spanned by the generalized eigenvectors associated to the first eigenvalue.

Proposition 1. *The system* (1) *can be stabilized along the eigenspace associated to its first eigenvalue* λ_1*, through the feedback control action*

$$\tau = -\beta M \left(V \begin{bmatrix} 0_{m_1\times m_1} & 0_{m_1\times n-m_1} \\ 0_{n-m_1\times m_1} & \mathrm{I}_{n-m_1\times n-m_1} \end{bmatrix} V^{\mathrm{T}} \right) \dot{x}\,. \tag{2}$$

Each column of $V \in \mathbb{R}^{n\times n}$ *is a distinct generalized eigenvector of the matrix* $M^{-1}K$ *in* (1)*, ordered such that the first* m_1 *left columns are a base of the eigenspace associated to* λ_1*.*

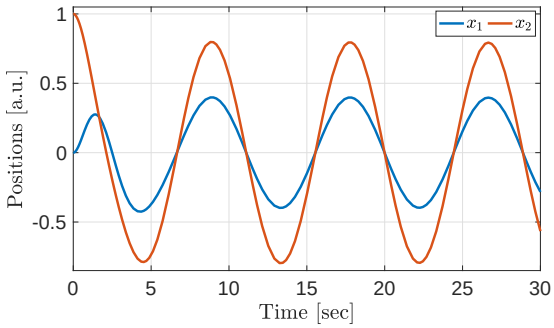

(a)

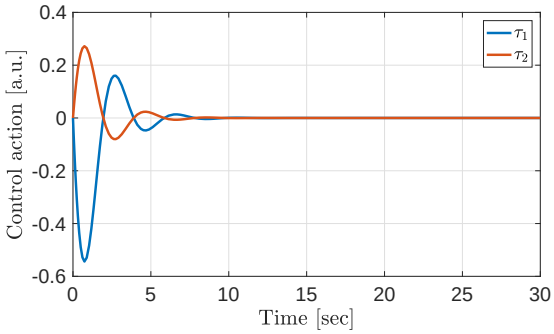

(b)

Figure 3. Panel (a) shows the evolution of system (3), controlled through (5), for the initial conditions $x_1(0) = 0$, $x_2(0) = 1$a.u., $\dot{x}_1(0) = 0$, $\dot{x}_2(0) = 0$. Panel (b) shows the corresponding evolution of the control action. After about 10s the system converges to the desired modal oscillation. From there on the robot has no need of extra energy injection to follow the desired trajectory.

$\mathrm{I}_{n-1\times n-1} \in \mathbb{R}^{n-1\times n-1}$ *is the identity matrix,* $0_{m_1\times m_1} \in \mathbb{R}^{m_1\times m_1}$, $0_{m_1\times n-m_1} \in \mathbb{R}^{m_1\times n-m_1}$, $0_{n-m_1\times m_1} \in \mathbb{R}^{n-m_1\times m_1}$ *are null matrices,* m_1 *is the algebraic multiplicity of* λ_1*, and* $\beta \in \mathbb{R}^+$ *is a positive constant.*

Proof. Please refer to Appendix A for the proof of this proposition. □

Lets consider as an example the linear system in Fig. 2. We describe it through the following set of linear ordinary differential equations

$$\begin{bmatrix} m_1\ddot{x}_1 \\ m_2\ddot{x}_2 \end{bmatrix} = \begin{bmatrix} -k_1-k_2 & k_2 \\ k_2 & -k_2 \end{bmatrix} \begin{bmatrix} x_1 \\ x_2 \end{bmatrix} + \begin{bmatrix} \tau_1 \\ \tau_2 \end{bmatrix}, \tag{3}$$

where x_1 and x_2 are the positions of the two bodies, k_1 and k_2 are the stiffnesses of the springs, m_1 and m_2 are the body masses. Two forces τ_1 and τ_2 can be exerted on the bodies. For the sake of simplification we fix $m_1 = 1$ a.u., $m_2 = 1$ a.u., and $k_2 = 1$ a.u.. The two directions of modal oscillation in configuration space are the columns of the matrix

$$V = \begin{bmatrix} \frac{\sqrt{{k_1}^2+4}}{2} - \frac{k_1}{2} & -\frac{\sqrt{{k_1}^2+4}}{2} - \frac{k_1}{2} \\ 1 & 1 \end{bmatrix}. \tag{4}$$

The first column describes an in-phase motion, while the second one describes a motion in phase opposition. Through proper choice of the physical stiffness k_1, a vast range of modal oscillations can be implemented. Consider for instance an oscillation for the second body with double the amplitude w.r.t. the first one. This can be obtained by fixing $k_1 = \frac{3}{2}$a.u.. Applying now the control strategy (2), yields the following feedback law

$$\begin{bmatrix} \tau_1 \\ \tau_2 \end{bmatrix} = \begin{bmatrix} -1 & \frac{1}{2} \\ \frac{1}{2} & -\frac{1}{4} \end{bmatrix} \begin{bmatrix} \dot{x}_1 \\ \dot{x}_2 \end{bmatrix}, \tag{5}$$

where $\beta = \frac{5}{4}$a.u.. In this way, the system evolves along the second mode as a damped oscillator, eventually converging to a stable oscillation in the direction described by the first column of V. The resulting closed loop behavior is presented in Fig. 3. After about 10s the system reaches the desired oscillatory behavior, evolving without the need of any extra energy injection from there on out.

Of course the linear case is easy to address. However, applications where oscillations of a linear mechanical system could be practically exploited are relatively few in robotics. As discussed above, moving instead from linear to the nonlinear domain, many important applications can be included. On the other hand, the analysis, design and control problems become much harder, and even defining normal modes turns into a challenging task.

III. Nonlinear Normal Modes

A. Background

Lets consider a generic nonlinear mechanical system with n degrees of freedom in the form

$$\ddot{x}_j = f_j(x,\dot{x}), \tag{6}$$

where $x = [x_1,\ldots,x_n] \in \mathbb{R}^n$ are the system configuration coordinates, $\dot{x} = [\dot{x}_1,\ldots,\dot{x}_n] \in \mathbb{R}^n$ their derivatives, and $f_j(x,\dot{x}) : \mathbb{R}^{2n} \to \mathbb{R}$ is the dynamics of the $j-$th DoF.

Generalizing the powerful linear modal analysis to nonlinear mechanical systems occupies the dynamical system theorists since Lyapunov times (see e.g. [37]). In his seminal work [38], Rosenberg defines a nonlinear normal mode as "*vibrations in unison*" where all the material points of the system reach their extremal points and cross the origin simultaneously. The modes are called *similar* or rectilinear if they move in a flat space, and *non-similar* otherwise. While similar normal modes are not typical in nonlinear systems, nontrivial examples exist in literature [39], [30]. Non-similar Normal Modes are well studied, e.g. from the point of view of resonances [40], localization [41], and bifurcations [42]. However Rosenberg's definition has two major limitations: i) in resonant conditions the relative phases of the oscillations can change, violating the unison hypothesis; ii) it requires the system to be conservative.

In their 1993 work [43], Shaw and Pierre proposed an alternative extension of linear modes overcoming these limitations, by generalizing eigenspaces to curvilinear spaces through the concept of invariant manifolds. A manifold is invariant w.r.t a dynamics, if the vector field describing the system dynamics is always tangent to the manifold, i.e. if a trajectory initialized on the manifold remains on it. As discussed in the previous section, this invariance property is a main characteristics of eigenspaces in linear system, which are thus invariant manifold.

Shaw-Pierre Nonlinear Normal Modes (NNM) were defined as "*a motion which takes place on a two-dimensional invariant*

manifold in the system's phase space", which is tangent to an eigenspace of the linearized system in an equilibium point. We will refer in the following to such invariant manifold, as *modal manifold*.

For the sake of brevity and clarity, we introduce the following common assumptions

i We consider the modal manifold to be parameterizable through two independent variables [44], which are typically selected as one configuration coordinate and its time derivative [43].
ii We select $x_1, \dot{x}_1$ as independent variables.
iii We assume the system equilibrium to be such that $x_1 = 0$.

Note that the first assumption constraints the NNM to be a continuation of a linear mode unidimensional in configuration space. In other words, the algebraic multiplicity m_1 of the first eigenvalues λ_1 of the linearized system is equal to 1. Second and third assumptions are instead imposed without loss of generality. It is convenient, but not necessary, to perform a linear change of variables such that x_1 points in the direction of modal oscillation, as e.g. in (54).

Under these three assumptions the manifold can be implicitly defined by the set of nonlinear algebraic equations[1]

$$x_j = X_j(x_1, \dot{x}_1)\,, \quad \dot{x}_j = \dot{X}_j(x_1, \dot{x}_1) \qquad \forall j \in \{1 \dots n\}\,, \tag{7}$$

where $X_j : \mathbb{R}^2 \to \mathbb{R}$ and $\dot{X}_j : \mathbb{R}^2 \to \mathbb{R}$ $\forall j \in \{1 \dots n\}$ (hereinafter also called maps). For $j = 1$ the maps have the trivial forms $X_1(x_1, \dot{x}_1) = x_1$ and $\dot{X}_1(x_1, \dot{x}_1) = \dot{x}_1$. Using (7), the dynamics of x_1 on the manifold can be expressed independently from the values of $x_2, \dots, x_n$ as

$$\begin{cases} \ddot{x}_1 = F_{\mathrm{m}}(x_1, \dot{x}_1) \\ F_{\mathrm{m}}(x_1, \dot{x}_1) \triangleq f_1(X(x_1, \dot{x}_1), \dot{X}(x_1, \dot{x}_1))\,, \end{cases} \tag{8}$$

where $X(x_1, \dot{x}_1) : \mathbb{R}^2 \to \mathbb{R}^{2n}$ and $\dot{X}(x_1, \dot{x}_1) : \mathbb{R}^2 \to \mathbb{R}^{2n}$ are vector valued functions having as $j-$th element X_j and $\dot{X}_j$ respectively, and $F_{\mathrm{m}}(\cdot, \cdot)$ specifies the modal dynamics.

Thus, if initialized on the modal manifold the mechanical system is equivalent to the one dimensional dynamics (8), which drives the remaining $n-1$ degrees of freedom through the set of algebraic relationships (7). This resembles the behavior of a linear system initialized on one of its eigenspaces. We summarize such physical interpretation in Fig. 4. To further underline this distinction, in literature x_1 is referred as master variable, and $x_2, \dots, x_n$ as slave variables.

B. Evaluation of the Invariant Manifold

The manifold geometry can be connected to the system dynamics by deriving (7), and substituting the vector field (6) on the manifold. This yields to the set of tangency constraints

$$\begin{aligned} \dot{X}_j &= \frac{\partial X_j}{\partial x_1}\dot{x}_1 + \frac{\partial X_j}{\partial \dot{x}_1} f_1(X, \dot{X}) \\ f_j(X, \dot{X}) &= \frac{\partial \dot{X}_j}{\partial x_1}\dot{x}_1 + \frac{\partial \dot{X}_j}{\partial \dot{x}_1} f_1(X, \dot{X}) \end{aligned} \qquad \forall j \in \{2 \dots n\}\,, \tag{9}$$

[1]Note that the dot on top of $\dot{X}$ should not be considered as a time derivation. This abuse of notation is instrumental to simplify the notation afterwards.

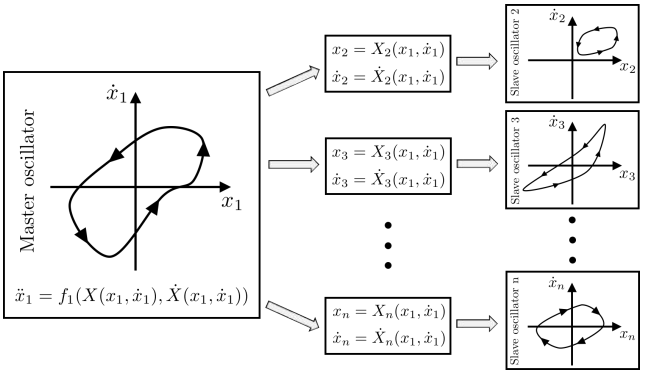

Figure 4. If initialized on the invariant manifold, the evolution of the system is fully defined by the one dimensional dynamics of the master variable. The remaining $n-1$ slave variables are specified by the master variable through a set of nonlinear algebraic functions.

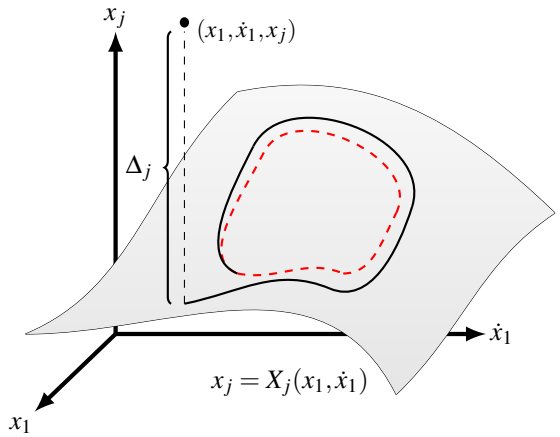

Figure 5. Representation of the NNM control problem for the $j-th$ configuration coordinate x_j. We considered two control goals: i) making the manifold attractive, i.e. assure that Δ_j tends to 0; ii) injecting or removing energy in order to change the amplitude of oscillation.

where we omitted the dependency of X and $\dot{X}$ on $x_1, \dot{x}_1$. We are also not considering the trivial case of $j = 1$, that automatically holds. This set of $2(n-1)$ nonlinear partial differential equations is hardly solvable in the general case, as also pointed out by Shaw and Pierre in [43]. As alternative to the exact solution of (9) two approaches exist in literature. One is to search for analytical approximated solutions in the Galerkin sense [45]. The basic idea is to apply some constraints on the functional spaces in which $X_j, \dot{X}_j, f_j$ live, to express them with a finite set of basis functions. This allows to approximate the PDEs with a set of algebraic equations. Approaches of this type that were employed so far are Taylor expansion [43], Koopman operator [46], and Harmonic balance [47]. In alternative to this approach, several numerical methods were proposed in literature, as e.g. finite element analyses. See [48] for an extensive review. The result is a numerical approximation of the PDE solution. For further details on theoretical and applicative results in Nonlinear Normal Modes please refer to [29] and [49] respectively.

IV. Controlling Nonlinear Normal Modes

As discussed in Sec. II for the linear case, we propose here to generate efficient nonlinear oscillations in soft robots by stabilizing a modal invariant manifold, which thus assumes the role of an artificial counterpart of the natural UCM [26]. We will also briefly discuss the problem of injecting or removing energy in the system, in order increase or decrease the amplitude of modal oscillations.

A. General model definition

Accordingly to the standard formulation in [50], a generic soft robot can be modeled as

$$\begin{bmatrix} M(x_\mathrm{r},x_\mathrm{m}) & Q(x_\mathrm{r},x_\mathrm{m}) \\ Q^\mathrm{T}(x_\mathrm{r},x_\mathrm{m}) & B(x_\mathrm{r},x_\mathrm{m}) \end{bmatrix} \begin{bmatrix} \ddot{x}_\mathrm{r} \\ \ddot{x}_\mathrm{m} \end{bmatrix} + c(x_\mathrm{r},x_\mathrm{m},\dot{x}_\mathrm{r},\dot{x}_\mathrm{m}) + g(x_\mathrm{r},x_\mathrm{m}) + \begin{bmatrix} \frac{\partial V(x_\mathrm{r},x_\mathrm{m})}{\partial x_\mathrm{r}} \\ \frac{\partial V(x_\mathrm{r},x_\mathrm{m})}{\partial x_\mathrm{m}} \end{bmatrix} + d(x_\mathrm{r},x_\mathrm{m}) = \begin{bmatrix} \tau_\mathrm{r} \\ \tau_\mathrm{m} \end{bmatrix} \tag{10}$$

where x_m are the configuration coordinates associated to the motors, and x_r is the robot configuration. $M(x_\mathrm{r},x_\mathrm{m})$, $B(x_\mathrm{r},x_\mathrm{m})$ and $Q(x_\mathrm{r},x_\mathrm{m})$ are inertia matrices of links, motors and coupling respectively. $c(x_\mathrm{r},x_\mathrm{m},\dot{x}_\mathrm{r},\dot{x}_\mathrm{m})$ collects Coriolis and centrifugal effects. $g(x_\mathrm{r},x_\mathrm{m})$ models the gravity torque, and $V(x_\mathrm{r},x_\mathrm{m})$ is the elastic potential. τ_r and τ_m are the actuations. Note that, while formulated with articulated soft robots in mind, this definition also includes discrete models of continuous soft robots [32], [34].

By considering $x = \begin{bmatrix} x_\mathrm{r}^\mathrm{T} & x_\mathrm{m}^\mathrm{T} \end{bmatrix}^\mathrm{T}$,

$$\tau = \begin{bmatrix} M(x_\mathrm{r},x_\mathrm{m}) & Q(x_\mathrm{r},x_\mathrm{m}) \\ Q^\mathrm{T}(x_\mathrm{r},x_\mathrm{m}) & B(x_\mathrm{r},x_\mathrm{m}) \end{bmatrix}^{-1} \begin{bmatrix} \tau_\mathrm{r} \\ \tau_\mathrm{m} \end{bmatrix}, \tag{11}$$

and

$$f(x,\dot{x}) = -\begin{bmatrix} M(x_\mathrm{r},x_\mathrm{m}) & Q(x_\mathrm{r},x_\mathrm{m}) \\ Q^\mathrm{T}(x_\mathrm{r},x_\mathrm{m}) & B(x_\mathrm{r},x_\mathrm{m}) \end{bmatrix}^{-1} (c(x_\mathrm{r},x_\mathrm{m},\dot{x}_\mathrm{r},\dot{x}_\mathrm{m}) + g(x_\mathrm{r},x_\mathrm{m}) + \begin{bmatrix} \frac{\partial V(x_\mathrm{r},x_\mathrm{m})}{\partial x_\mathrm{r}} \\ \frac{\partial V(x_\mathrm{r},x_\mathrm{m})}{\partial x_\mathrm{m}} \end{bmatrix} + d(x_\mathrm{r},x_\mathrm{m})), \tag{12}$$

Eq. (10) is rewritten as the actuated version of the generic nonlinear mechanical system (6). Thus the dynamical model of the $j-$th configuration coordinates of a soft robot that we consider in the following is

$$\ddot{x}_j = f_j(x,\dot{x}) + \tau_j, \tag{13}$$

where $\ddot{x}_j$, $\dot{x}_j$,x_j, τ_j, and f_j are the $j-$th elements of $\ddot{x}$, $\dot{x}$,x, τ, and f respectively.

We introduce $\Sigma : \mathbb{R}^2 \to \mathbb{R}^{n-1\times n-1}$ and $\Gamma : \mathbb{R}^2 \to \mathbb{R}^{n-1\times n-1}$, with elements (i,j) defined as

$$\Sigma_{i,j}(x_1,\dot{x}_1) = \left.\frac{\partial f_{i+1}}{\partial x_{j+1}}\right|_{x=X,\dot{x}=\dot{X}} \qquad \Gamma_{i,j}(x_1,\dot{x}_1) = \left.\frac{\partial f_{i+1}}{\partial \dot{x}_{j+1}}\right|_{x=X,\dot{x}=\dot{X}}. \tag{14}$$

These two matrix-valued functions generalize the role that damping and stiffness had in the linear case. Note indeed that $\Sigma(0,0)$ is the stiffness of the slave variables in the equilibrium point, and $\Gamma(0,0)$ the damping.

We refer the total energy of the soft robot (13) as $E(x,\dot{x})$. We also define the equivalent energy on the manifold as

$$E_\mathrm{M}(x_1,\dot{x}_1) = E(X(x_1,\dot{x}_1),\dot{X}(x_1,\dot{x}_1)). \tag{15}$$

B. Stabilization

In this work we consider the following definition of manifold stability

Definition 1. *Given a manifold parametrized by the two maps $X(x_1,\dot{x}_1)$ and $\dot{X}(x_1,\dot{x}_1)$ in (7), we call it locally attractive if $\exists\delta > 0$ such that if $x_j(0),\dot{x}_j(0)\ \forall j \in \{1\dots n\}$ are such that $||x_i(0)-X_i(x_1(0),\dot{x}_1(0))|| + ||\dot{x}_i(0)-\dot{X}_i(x_1(0),\dot{x}_1(0))|| < \delta\ \forall i \in \{1\dots n\}$, then it holds*

$$\lim_{t\to\infty} x_i(t) - X_i(x_1(t),\dot{x}_1(t)) = 0 \qquad \lim_{t\to\infty} \dot{x}_i(t) - \dot{X}_i(x_1(t),\dot{x}_1(t)) = 0 \qquad \forall i \in \{1,\dots,n\}. \tag{16}$$

The following theorem generalizes Proposition 1 to the nonlinear case, providing a control strategy able to regulate the soft robot on one of its modal manifolds.

Theorem 1. *Let $X(x_1,\dot{x}_1)$ and $\dot{X}(x_1,\dot{x}_1)$ be the parametrization of a nonlinear modal manifold for the n-DoF nonlinear mechanical system* (6)*.*

Then the feedback law

$$\tau(x,\dot{x}) = -\begin{bmatrix} 0 & 0 \\ 0 & \mathrm{I}_{n-1} \end{bmatrix} (\kappa_\mathrm{p}\Delta + \kappa_\mathrm{d}\dot{\Delta}) + \begin{bmatrix} \tau_1(x,\dot{x}) \\ 0 \\ \vdots \\ 0 \end{bmatrix}, \tag{17}$$

where $\kappa_\mathrm{p} \in \mathbb{R}^+$, $\kappa_\mathrm{d} \in \mathbb{R}^+$, $\Delta = X(x_1,\dot{x}_1) - x$, and

$$\tau_1(x,\dot{x}) = f_1(X(x_1,\dot{x}_1),\dot{X}(x_1,\dot{x}_1)) - f_1(x,\dot{x}), \tag{18}$$

preserves the invariance of the manifold.

Furthermore, the two following sufficient conditions for the local attractiveness hold

i) *$\delta \in \mathbb{R}^+$ always exists such that if*

$$||\dot{\Sigma}(x_1,\dot{x}_1)|| < \delta, \quad ||\dot{\Gamma}(x_1,\dot{x}_1)|| < \delta$$

then the manifold is attractive $\forall \kappa_\mathrm{p},\kappa_\mathrm{d}$ such that

$$\lambda^-(\Sigma(x_1,\dot{x}_1)) > -\kappa_\mathrm{p}, \quad \lambda^-(\Gamma(x_1,\dot{x}_1)) > -\kappa_\mathrm{p},$$

where $\lambda^-(\cdot)$ is the minimum eigenvalue of the argument.

ii) *If $\Sigma(x_1,\dot{x}_1)$ and $\Gamma(x_1,\dot{x}_1)$ are simultaneously diagonalizable by a matrix $\mu(x_1,\dot{x}_1) \in \mathbb{R}^{n-1\times n-1}$, then the manifold is attractive if*

$$\lambda_i(\Sigma(x_1,\dot{x}_1)) > -\kappa_\mathrm{p} \qquad \lambda_i(\Gamma(x_1,\dot{x}_1)) > -\kappa_\mathrm{d} - \frac{\lambda_i(\dot{\Sigma}(x_1,\dot{x}_1))}{\lambda_i(\Sigma(x_1,\dot{x}_1)) - \kappa_\mathrm{p}} \tag{19}$$

where $\lambda_i(\cdot)$ extracts the eigenvalue corresponding to the $i-th$ column of $\mu(x_1,\dot{x}_1)$.

Proof. On the manifold (i.e. when $x_i = X_i(x_1,\dot{x}_1)$ and $\dot{x}_i = \dot{X}_i(x_1,\dot{x}_1)$) $\tau_1 \equiv 0$ and $\tau_j \equiv 0$. Thus, condition (9) is identical for the actuated and not actuated system, which proves the first thesis.

To prove the attractiveness, we define the displacement w.r.t. the manifold as (see Fig. 5)

$$\Delta_j \triangleq X_j(x_1,\dot{x}_1) - x_j\,. \tag{20}$$

Deriving w.r.t. time yields

$$\begin{aligned}\dot{\Delta}_j &= -\dot{x}_j + \frac{\partial X_j}{\partial x_1}\dot{x}_1 + \frac{\partial X_j}{\partial \dot{x}_1}[f_1(x,\dot{x}) + \tau_1] \\ &= -\dot{x}_j + \dot{X}(x_1,\dot{x}_1) + \frac{\partial X_j}{\partial \dot{x}_1}[f_1(x,\dot{x}) - f_1(X,\dot{X}) + \tau_1]\,,\end{aligned} \tag{21}$$

where in the first step we used the chain rule, and in the second step we used (9), i.e. the manifold invariance. Now, we close the loop with (18) obtaining

$$\dot{\Delta}_j = \dot{X}_j(x_1,\dot{x}_1) - \dot{x}_j\,, \tag{22}$$

which now describes the displacement between velocities and corresponding manifold coordinate. We derive (22) a second time obtaining

$$\begin{aligned}\ddot{\Delta}_j &= -f_j(x,\dot{x}) - \tau_j + \frac{\partial \dot{X}_j}{\partial x_1}\dot{x}_1 + \frac{\partial \dot{X}_j}{\partial \dot{x}_1}[f_1(x,\dot{x}) + \tau_1] \\ &= -f_j(x,\dot{x}) - \tau_j + \frac{\partial \dot{X}_j}{\partial x_1}\dot{x}_1 + \frac{\partial \dot{X}_j}{\partial \dot{x}_1} f_1(X(x_1,\dot{x}_1),\dot{X}(x_1,\dot{x}_1))\,,\end{aligned} \tag{23}$$

taking again the control (18) into account. Now, by exploiting the manifold invariance and substituting (20) and (22), we write

$$\begin{aligned}\ddot{\Delta}_j = {} & f_j(X(x_1,\dot{x}_1),\dot{X}(x_1,\dot{x}_1)) \\ & - f_j(X(x_1,\dot{x}_1) - \Delta, \dot{X}(x_1,\dot{x}_1) - \dot{\Delta}) - \tau_j\,.\end{aligned} \tag{24}$$

To complete the proof we linearize the dynamics around a generic equilibrium trajectory on the manifold, i.e. for $\Delta_j = 0$ and $\dot{\Delta}_j = 0\ \forall j \in \{2\dots n\}$

$$\begin{bmatrix}\dot{\xi}\\ \ddot{\xi}\end{bmatrix} \simeq \begin{bmatrix}0 & I\\ -(\Sigma(x_1,\dot{x}_1) + \kappa_\mathrm{p}\mathrm{I}) & -(\Gamma(x_1,\dot{x}_1) + \kappa_\mathrm{d}\mathrm{I}))\end{bmatrix}\begin{bmatrix}\xi\\ \dot{\xi}\end{bmatrix}\,, \tag{25}$$

where $\xi = \begin{bmatrix}\Delta_2 \dots \Delta_n\end{bmatrix}^\mathrm{T}$ and $\dot{\xi} = \begin{bmatrix}\dot{\Delta}_2 \dots \dot{\Delta}_n\end{bmatrix}^\mathrm{T}$, and where we exploited that $\Delta_1 \equiv 0$ and $\dot{\Delta}_1 \equiv 0$ by construction. In (25), x_1 and $\dot{x}_1$ do not appear as an input, but only as dependencies in the dynamic matrix. Indeed it holds

$$\frac{\partial f_j(x_1,\dot{x}_1,X_2\dots\dot{X}_n)}{\partial x_1} = \left.\frac{\partial f_j(x_1,\dot{x}_1,X_2-\Delta_2\dots\dot{X}_n-\dot{\Delta}_n)}{\partial x_1}\right|_{\substack{\Delta_j=0\\ \dot{\Delta}_j=0}} \tag{26}$$

$$\frac{\partial f_j(x_1,\dot{x}_1,X_2\dots\dot{X}_n)}{\partial \dot{x}_1} = \left.\frac{\partial f_j(x_1,\dot{x}_1,X_2-\Delta_2\dots\dot{X}_n-\dot{\Delta}_n)}{\partial \dot{x}_1}\right|_{\substack{\Delta_j=0\\ \dot{\Delta}_j=0}}\,. \tag{27}$$

Note that the controller τ_1 decouples the dynamics of master variable from the slave variables. Indeed it holds $\ddot{x}_1 = f_1(x,\dot{x}) + (f_1(X(x_1,\dot{x}_1),\dot{X}(x_1,\dot{x}_1)) - f_1(x,\dot{x})) = f_1(X(x_1,\dot{x}_1),\dot{X}(x_1,\dot{x}_1))$, i.e. x_1 evolves accordingly to the modal dynamics (8) also outside the manifold. Thus, the dependency of Eq. (25) from x_1 and $\dot{x}_1$ can be regarded as a time-variance, and (i) is directly proven by applying the Lemma 1 in appendix B.

For proving (ii), we consider that two matrices are simultaneous diagonalizable if and only if they commute [51]. Hence, the hypothesis of simultaneous diagonalizability of Σ and Γ implies that they commute, which in turn assures that also $\Sigma(x_1,\dot{x}_1) + \kappa_\mathrm{p}\mathrm{I}$ and $\Gamma(x_1,\dot{x}_1) + \kappa_\mathrm{d}\mathrm{I}$ commute

$$\begin{aligned}&(\Sigma(x_1,\dot{x}_1) + \kappa_\mathrm{p}\mathrm{I})\,(\Gamma(x_1,\dot{x}_1) + \kappa_\mathrm{d}\mathrm{I}) \\ =&\Sigma(x_1,\dot{x}_1)\Gamma(x_1,\dot{x}_1) + \Sigma(x_1,\dot{x}_1)\kappa_\mathrm{d} + \kappa_\mathrm{p}\Gamma(x_1,\dot{x}_1) + \kappa_\mathrm{p}\kappa_\mathrm{d}\mathrm{I} \\ =&\Gamma(x_1,\dot{x}_1)\Sigma(x_1,\dot{x}_1) + \kappa_\mathrm{d}\Sigma(x_1,\dot{x}_1) + \Gamma(x_1,\dot{x}_1)\,\kappa_\mathrm{p} + \kappa_\mathrm{d}\kappa_\mathrm{p}\mathrm{I} \\ =&(\Gamma(x_1,\dot{x}_1) + \kappa_\mathrm{d}\mathrm{I})\,(\Sigma(x_1,\dot{x}_1) + \kappa_\mathrm{p}\mathrm{I})\,.\end{aligned} \tag{28}$$

Thus the thesis results from the application of Lemma 2 in appendix B, considering the hypothesis (19).

□

The proposed control law (17) is indeed a nonlinear generalization of (2):

a) If $\Sigma \prec 0$ the damping injection is sufficient to stabilize the manifold, i.e. $\kappa_\mathrm{p} = 0$, as in the linear case.
b) We need here the extra control action $\tau_1 = f_1(X,\dot{X}) - f_1(x,\dot{x})$, which is essentially non-local. Indeed, due to the tangency property of the modal invariant manifold, in the case of x_1 pointing in the direction of the first eigenvector of the linearized system, $\frac{\partial \tau_1}{\partial x_1}\big|_{x_1=0,\dot{x}_1=0} = 0$ and $\frac{\partial \tau_1}{\partial \dot{x}_1}\big|_{x_1=0,\dot{x}_1=0} = 0$.
c) Note also that we are expressing the control in modal coordinates (i.e. x_1 master variable) for the sake of clarity and conciseness. Thus no change of coordinates (cf. V in (2)) explicitly appears in (17). It should also be noticed that the pre-multiplications for the inertia matrix present in (2) are happening implicitly in the non linear case through (11) and (12).

C. Orbit excitation

In this section we investigate the possibility of injecting or removing energy in order to increase or decrease the amplitude of oscillation. To this end, we start by asking under which conditions it is possible to generate a control action $\tau(x,\dot{x})$, that does not vanish on the manifold (i.e. $\tau(X,\dot{X}) \neq 0$) and such that the closed loop manifold is parametrized by the same maps X and $\dot{X}$ of the open loop one. This is equivalent to impose that both (6) and (13) verify (9) for a same X and $\dot{X}$. So, lets start by considering the second set of equations in (9),

$$\begin{cases} f_j(X,\dot{X}) = \frac{\partial \dot{X}_j}{\partial x_1}\dot{x}_1 + \frac{\partial \dot{X}_j}{\partial \dot{x}_1} f_1(X,\dot{X}) \\ f_j(X,\dot{X}) + \tau_j(X,\dot{X}) = \frac{\partial \dot{X}_j}{\partial x_1}\dot{x}_1 + \frac{\partial \dot{X}_j}{\partial \dot{x}_1}(f_1(X,\dot{X}) + \tau_1(X,\dot{X}))\,,\end{cases} \tag{29}$$

where τ_j is the $j-th$ element of τ. By subtracting the first equation from the second, the following condition results

$$\tau_j = \frac{\partial \dot{X}_j}{\partial \dot{x}_1}\tau_1\,, \tag{30}$$

which prescribes how to exert τ_j, given τ_1.

Lets consider now the first equation in (9), for the two systems (6) and (13)

$$\begin{cases}\dot{X}_j = \frac{\partial X_j}{\partial x_1}\dot{x}_1 + \frac{\partial X_j}{\partial \dot{x}_1} f_1(X,\dot{X}) \\ \dot{X}_j = \frac{\partial \dot{X}_j}{\partial x_1}\dot{x}_1 + \frac{\partial \dot{X}_j}{\partial \dot{x}_1}(f_1(X,\dot{X}) + \tau_1(X,\dot{X}))\,.\end{cases} \tag{31}$$

Subtracting the two yields

$$\frac{\partial X_j}{\partial \dot{x}_j}\,\tau_1 \equiv 0 \quad \forall j\,. \tag{32}$$

This equation leads to two possible scenarios. If

$$\frac{\partial X_j}{\partial \dot{x}_j} \equiv 0\,, \tag{33}$$

then τ_1 can be freely exerted. Note that (33) means $x_j = X_j(x_1)$, i.e. the manifold is described by a set of virtual holonomic constraints. In this case exerting τ such that (30) holds would be sufficient to inject energy into the system without ruining the invariance of the modal manifold.

However, this circumstance is rather restrictive. For this reason we will not consider it further in the paper. Under this assumption, (32) leads to $\tau_1 \equiv 0$, which in turn leads to $\tau_j \equiv 0$ $\forall j \in \{2 \dots n\}$ through (30). Thus exerting any generalized force always pushes the system away from the manifold.

Adopting the philosophy of [52], the following theorem proposes a simple extension of the stabilizing controller of Theorem 1, which is able to regulate the system energy within a certain interval despite the discussed limitations.

Theorem 2. *Lets consider the soft robot* (13)*, with a modal manifold parametrized by $X(x_1,\dot{x}_1)$ and $\dot{X}(x_1,\dot{x}_1)$, controlled through the feedback law*

$$\tau(x,\dot{x}) = -\begin{bmatrix} 0 & 0 \\ 0 & \mathrm{I}_{n-1} \end{bmatrix} (\kappa_\mathrm{p}\,\Delta + \kappa_\mathrm{d}\,\dot{\Delta}) + \begin{bmatrix} \tau_1(x,\dot{x}) + \bar{\tau}_1(x_1,\dot{x}_1) \\ 0 \\ \vdots \\ 0 \end{bmatrix}, \tag{34}$$

with τ_1 as in (18)*, and*

$$\bar{\tau}_1 = \gamma \begin{cases} 0 & \text{if } x_1 \notin [x_1^-, x_1^+] \vee E_\mathrm{M} \in [E^-, E^+] \\ 1 & \text{if } x_1 \in [x_1^-, x_1^+] \wedge \\ & \quad ((E_\mathrm{M} < E^- \wedge \dot{x}_1 > 0) \vee (E_\mathrm{M} > E^+ \wedge \dot{x}_1 < 0)) \\ -1 & \text{otherwise} \end{cases} \tag{35}$$

where $\gamma > 0$, $E^+ > E^- > 0$, and $x_1^+ > 0 > x_1^-$ are scalar constants. If the following conditions hold simultaneously

H1 *the soft robot is conservative, i.e. $\frac{\mathrm{d}E}{\mathrm{d}t}\big|_{\tau \equiv 0} = 0$*
H2 *the level curves of E_M are closed*
H3 *$f_1(X(x_1,0),\dot{X}(x_1,0)) \neq 0 \quad \forall x_1 \notin [x_1^-, x_1^+]$ and $f_1(X(x_1,0),\dot{X}(x_1,0)) \neq \gamma \; \forall x_1 \in [x_1^-, x_1^+]$*
H4 *the hypotheses of Theorem 1 are verified*

then the invariant manifold is locally attractive and

$$\lim_{t\to\infty} E(x(t)) \in [E^-, E^+]\,.$$

Proof. We consider the case $E(x_1(0),\dot{x}_1(0)) < E^-$, also sketched in Fig. 6. The case $E(x_1(0),\dot{x}_1(0)) > E^+$ can be derived with similar arguments. For this initial condition the closed loop dynamics of the master variable is

$$\begin{aligned} \ddot{x}_1 &= f_1(X(x_1,\dot{x}_1),\dot{X}(x_1,\dot{x}_1)) \\ &\quad + \begin{cases} & 0 \quad \text{if } x_1 \notin [x_1^-, x_1^+] \\ + & \gamma \quad \text{if } x_1 \in [x_1^-, x_1^+] \wedge \dot{x}_1 > 0 \\ - & \gamma \quad \text{otherwise}\,, \end{cases} \end{aligned} \tag{36}$$

which is an autonomous dynamics, not depending on the evolution of slave variables $x_2 \dots x_n$. As common in the theory of hybrid systems [53], we make a partition of the time into a sequence of intervals

$$[0,t) = (\bigcup_1^{i^+(t)} t_i^\mathrm{in}) \cup (\bigcup_1^{j^+(t)} t_j^\mathrm{out}) \cup (\bigcup_1^{k^+(t)} t_k^0)\,, \tag{37}$$

where t_i^in is the $i-th$ interval for which $x_1 \in [x_1^-, x_1^+]$ and $\dot{x}_1 \neq 0$, t_j^out is the $j-th$ interval for which $x_1 \notin [x_1^-, x_1^+]$, t_k^0 is the $k-th$ interval for which $x_1 \in [x_1^-, x_1^+]$ and $\dot{x}_1 = 0$. $i^+(t), j^+(t), k^+(t)$ are the number of intervals $t_i^\mathrm{in}, t_j^\mathrm{out}, t_k^0$ contained $[0,t)$.

Conditions $x_1 \in [x_1^-, x_1^+]$ and $\dot{x}_1 = 0$ hold only for isolated instants, since H3 leads to $\ddot{x}_1 \neq 0$. Thus t_k^0 are all of zero measure.

If $x_1(t) \notin [x_1^-, x_1^+]$ then (36) becomes

$$\ddot{x}_1 = f_1(X(x_1,\dot{x}_1),\dot{X}(x_1,\dot{x}_1))\,,$$

which is the master variable's dynamics on the manifold (8). Thus H1 leads to

$$\frac{\mathrm{d}E_\mathrm{M}}{\mathrm{d}t} = 0 \Rightarrow \frac{\mathrm{d}E_\mathrm{M}}{\mathrm{d}x_1}\dot{x}_1 + \frac{\mathrm{d}E_\mathrm{M}}{\mathrm{d}\dot{x}_1}\ddot{x}_1 = 0\,, \tag{38}$$

i.e. x_1 evolves on the level curves of E_M. This, in combination with H2, implies that its orbits intercept the interval $[x_1^-, x_1^+]$. Finally H3 assures that (8) has no equilibria on the orbit, i.e. that the evolution of x_1 reaches the interval $[x_1^-, x_1^+]$ in finite time. So each t_j^out is finite, and it is always followed by a t_i^in.

Finally, when $x_1 \in [x_1^-, x_1^+]$ and $\dot{x}_1 \neq 0$, (36) is excited by a nonconservative force. This implies a energy change equal to

$$\begin{aligned} \frac{\mathrm{d}E_\mathrm{M}}{\mathrm{d}t}(x_1,\dot{x}_1) &= \dot{x}_1 \begin{cases} +\gamma & \text{if } \dot{x}_1 > 0 \\ -\gamma & \text{otherwise} \end{cases} \\ &= \gamma |\dot{x}_1| \geq \varepsilon > 0\,, \qquad \forall t \in t_i^\mathrm{in}\,. \end{aligned} \tag{39}$$

Thus

$$\begin{aligned} E_\mathrm{M}(t) &= E_\mathrm{M}(0) + \int_0^t \frac{\mathrm{d}E_\mathrm{M}}{\mathrm{d}t}\,\mathrm{d}t' \\ &= E_\mathrm{M}(0) + \int_0^{\bar{t}} \frac{\mathrm{d}E_\mathrm{M}}{\mathrm{d}t}\,\mathrm{d}t'' \\ &\geq E_\mathrm{M}(0) + \varepsilon \bar{t} \end{aligned} \tag{40}$$

where $\bar{t} = \sum_1^{i^+(t)} \max(t_i^\mathrm{in})$, and in the second step we changed the integral coordinate to express the time as union of t_i^in intervals.

Eq.s (39) and (40) imply that $E_\mathrm{M}(t)$ is increasing for $E_\mathrm{M} < E^-$. Thus x_1 and $\dot{x}_1$ eventually reach a value such that $E_\mathrm{M} = E^-$. H1 assures that the system in open loop is conservative, thus once reached this condition E_M remains in $[E^-, E^+]$.

Therefore a $T \in \mathbb{R}$ always exists such that $E_\mathrm{M}(x_1(t),\dot{x}_1(t)) \in [E^-, E^+]$ for all the $t > T$. This implies that $\bar{\tau}_1(x_1(t),\dot{x}_1(t)) = 0$, and (34) is equal to (17) for all the $t > T$. Invoking Theorem 1, the manifold attractiveness follows from H4, and in turn

$$\lim_{t\to\infty} E(x(t)) = \lim_{t\to\infty} E_\mathrm{M}(x_1(t),\dot{x}_1(t)) = E^- \in [E^-, E^+]\,.$$

□

Remark 1. *It is worth mentioning that both controllers* (17) *and* (34) *are such that $\tau_i \to 0$, since*

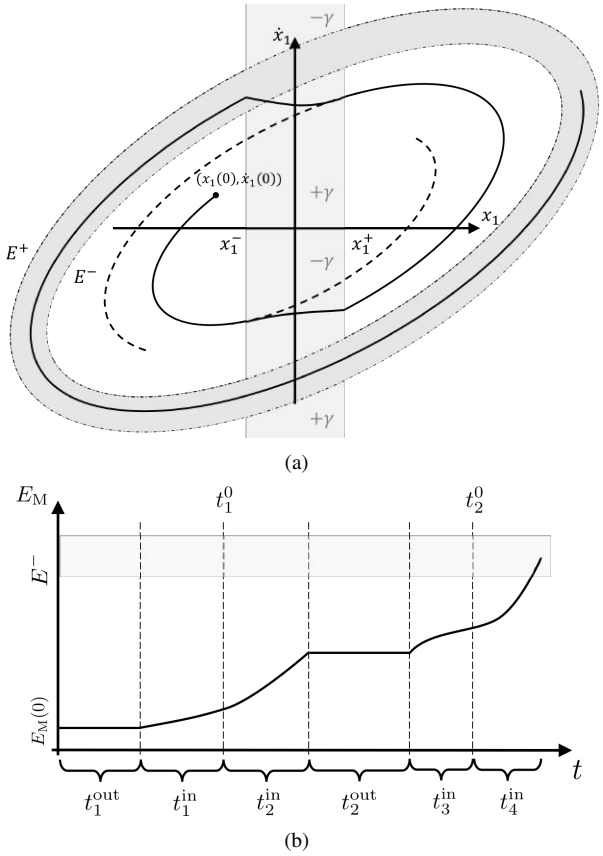

Figure 6. The master variable of a multi-DoF soft robot evolves under the control action (34). Panel (a) presents an evolution in the state space, while Panel (b) presents the corresponding evolution of the energy in time. When the system is in a neighborhood of equilibrium configuration $x_1 = 0$ (i.e. when it crosses the gray area), energy is injected by the controller, moving the system to another of its natural evolutions. Eventually this brings the soft robot in the region of state space with the desired amount of energy.

$\tau_i(x_1, \dot{x}_1, X_2, \dot{X}_2, \ldots, X_n, \dot{X}_n) \equiv 0$. *So they fulfill our main goal, i.e. that the system at steady state evolves in open loop without any injection of external energy.*

V. The Generalized SLIP Case of Study

In the following we present the application of the proposed strategy to a simple yet relevant example of soft robot: the radial elastic pendulum. This system generalize the so-called spring-loaded inverted pendulum (SLIP) by the introduction of a polar spring. From the bio-mechanical and robotic point of view, SLIP models assume a wide interest if considered that the center of mass evolution for legged animals can be generated as a trajectory of the SLIP model, both during running and walking gates [24], [54]. Existing control strategies implement locomotion by matching the robot dynamics to the SLIP one [21], [55].

A. Dynamical Model

The elastic pendulum model is

$$\begin{cases} \ddot{\theta} = -2\frac{\dot{r}}{r}\dot{\theta} + \frac{g}{r}\sin(\theta) - \frac{\kappa_1\theta}{r^2} \\ \ddot{r} = +r\dot{\theta}^2 - g\cos(\theta) - \kappa_2(r - r_0) \end{cases}, \tag{41}$$

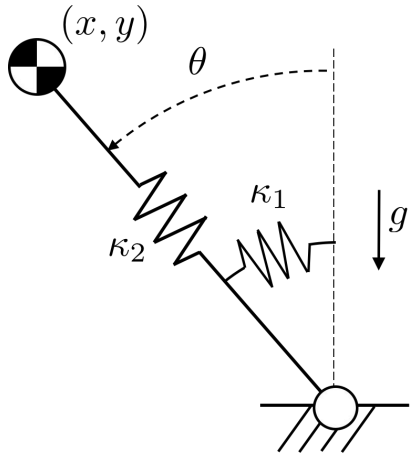

Figure 7. A sketch of the inverted elastic pendulum with main quantities underlined. In Cartesian coordinates the robot's pose is expressed by x and y, while θ and $r = \sqrt{x^2 + y^2}$ are the polar coordinates. κ_1 and κ_2 are a polar and a radial spring, normalized by the mass. κ_1 is equal to zero in the classic SLIP model. The mass is subjected to a constant gravitational field.

where θ and r are the polar coordinates of the body, with their derivatives $\dot{\theta}$, $\ddot{\theta}$, $\dot{r}$, $\ddot{r}$. g is the gravity constant. κ_1 and κ_2 are the ratio between spring stiffness and the body mass, i.e. what in the linear case would have been called natural frequencies of oscillation.

The system has an equilibrium in $\theta \equiv 0$ and $r \equiv r_0 - \frac{g}{\kappa_2}$. Its linearized dynamics is $\ddot{\theta} \simeq \frac{\kappa_1}{(r_0 - \frac{g}{\kappa_2})^2}\theta$, and $\ddot{\Delta r} \simeq -\kappa_2 \Delta r$. So, the linearized system normal modes are two decoupled evolutions along each degree of freedom: an angular oscillation with fixed radius, and a radial oscillation with fixed angle. The nonlinear extension of the latter radial mode remains a linear oscillation in the direction of the radial degree of freedom, since for $\theta \equiv 0$ and $\dot{\theta} \equiv 0$ the dynamics collapses into a linear one. The other mode instead turns into a much more complex oscillation which we investigate in the next subsections.

B. Analytical Approximated Solution of the Complete System

By considering as master variables $\theta, \dot{\theta}$, (9) and (41) yield

$$\begin{aligned} &\frac{\partial X}{\partial \theta}\dot{\theta} + \frac{\partial X}{\partial \dot{\theta}}(-2\frac{\dot{X}}{X}\dot{\theta} + \frac{g}{X}\sin(\theta) - \frac{\kappa_1\theta}{X^2}) = \dot{X} \\ &\frac{\partial \dot{X}}{\partial \theta}\dot{\theta} + \frac{\partial \dot{X}}{\partial \dot{\theta}}(-2\frac{\dot{X}}{X}\dot{\theta} + \frac{g}{X}\sin(\theta) - \frac{\kappa_1\theta}{X^2}) = X\dot{\theta}^2 - \kappa(X - r_0) \\ &\qquad\qquad - g\cos(\theta). \end{aligned} \tag{42}$$

where $X(\theta, \dot{\theta})$ and $\dot{X}(\theta, \dot{\theta})$ are the invariant manifold parametrization. We investigate the evaluation of the invariant manifold parametrization through the polynomial Galerkin method, as introduced in Sec. III. Upon their ability of locally approximating functions, polynomials have the advantage of being close w.r.t. derivation, product and sum. Thus, the solution can be found by i) approximating the dynamics as a reduced order polynomial, and guessing a polynomial form for X and $\dot{X}$, ii) substituting in (42), and evaluating the free parameters in X and $\dot{X}$ such that same order terms are equal.

Given a smooth function $f:\mathbb{R}^{2n}\to\mathbb{R}^n$, it is well known that its polynomial approximation can be evaluated as multivariate Taylor expansion. We consider here terms up to the third order

$$\begin{cases} \ddot\theta \simeq & -2\dot r\dot\theta(\frac{1}{r_0}-\frac{1}{r_0^2}(r-r_0)) \\ & +g(\frac{1}{r_0}-\frac{1}{r_0^2}(r-r_0)+\frac{1}{r_0^3}(r-r_0)^2)\theta-\frac{g}{6r_0}\theta^3 \\ & -\kappa_1(\frac{1}{r_0^2}-\frac{1}{r_0^3}(r-r_0)+\frac{1}{r_0^4}(r-r_0)^2)\theta \\ \ddot r \simeq & +r\dot\theta^2-g(1-\frac{\theta^2}{2})-\kappa_2(r-r_0)\,. \end{cases} \tag{43}$$

Regarding instead the maps X and $\dot X$, we start by considering the symmetry of Eq. (41), in θ w.r.t. 0. Indeed it is easy to realize that if $(\hat\theta,\ \dot{\hat\theta},\hat r,\dot{\hat r})$ is a system evolution, than also $(-\hat\theta,\ -\dot{\hat\theta},\hat r,\dot{\hat r})$ verifies the dynamics. This implies that X and $\dot X$ must be even, i.e. that their polynomial approximation does not present odd terms. As trade-off between complexity and accuracy we consider a forth order polynomial

$$\begin{bmatrix} X(\theta,\dot\theta) \\ \dot X(\theta,\dot\theta)\end{bmatrix} = \begin{bmatrix} r_0-\frac{g}{\kappa_2} \\ 0\end{bmatrix} + S(\theta,\dot\theta)\begin{bmatrix}\theta\\ \dot\theta\end{bmatrix} + F(\theta,\dot\theta)\begin{bmatrix}\theta\\ \dot\theta\end{bmatrix}, \tag{44}$$

with

$$S(\theta,\dot\theta)=\begin{bmatrix} a_3\,\theta+a_4\dot\theta & a_5\dot\theta \\ b_3\,\theta+b_4\dot\theta & b_5\dot\theta\end{bmatrix}$$

$$F(\theta,\dot\theta)=\begin{bmatrix} a_{10}\,\theta^3+a_{13}\,\dot\theta\,\theta^2+a_{12}\,\dot\theta^2\,\theta & a_{11}\,\dot\theta^2\,\theta+a_{14}\dot\theta^3 \\ b_{10}\,\theta^3+b_{13}\,\dot\theta\,\theta^2+b_{12}\,\dot\theta^2\,\theta & b_{11}\,\dot\theta^2\,\theta+b_{14}\dot\theta^3\end{bmatrix},$$

where a_i, b_i with $i\in\{3,4,5,10,11,12,13,14\}$ are the free parameters defining the geometry of the manifold. Introducing (43) and (44) into (42) yields 16 algebraic equations in the unknowns a_i, b_i, that we report in Appendix C. To solve them standard symbolic solvers can be employed (we used *solve* from `MatLab`). The solutions exist in closed form and they are ratios of two multivariate polynomial of the 15th order in the parameters κ_1, κ_2, g, r_0. We can not report their general form here for the sake of space, however Appendix D presents the case in which $r_0=1$m and $g=9.81\frac{\mathrm{Nm}}{\mathrm{s}^2}$. We obtain the mode dynamics by substituting the two maps in the $\ddot\theta$ dynamics

$$\ddot\theta=-2\frac{\dot X(\theta,\dot\theta)}{X(\theta,\dot\theta)}\dot\theta+\frac{gX(\theta,\dot\theta)\sin(\theta)-\kappa_1\,\theta}{X(\theta,\dot\theta)^2} \tag{45}$$

where the dependency of X and $\dot X$ on κ_1, κ_2, r_0, g is omitted.

C. Simulative Results

In order to obtain a convex oscillation (i.e. running-like) for all the considered angular velocities $\bar{\dot\theta}$, we set $\kappa_1=20\frac{1}{\mathrm{s}^2}$ and $\kappa_2=60\frac{1}{\mathrm{s}^2}$. Fig. 8 presents the modal trajectories of the system, superimposed at the corresponding tangent force field (i.e. (45)). Fig 9(a) and Fig. 9(b) present the manifold (i.e. respectively the maps X and $\dot X$), on which the orbits corresponding to the initial condition $\theta=0$ and $\dot\theta=\frac{\pi}{2}\frac{\mathrm{rad}}{\mathrm{s}}$ are drawn in solid line.

We consider now the application of the control law (17) to stabilize the manifold parametrized by X and $\dot X$. Note that, since the system has two degrees of freedom Σ and Γ (14) are scalars

$$\Sigma=\kappa_2-\dot\theta^2\,,\quad \Gamma=0\,. \tag{46}$$

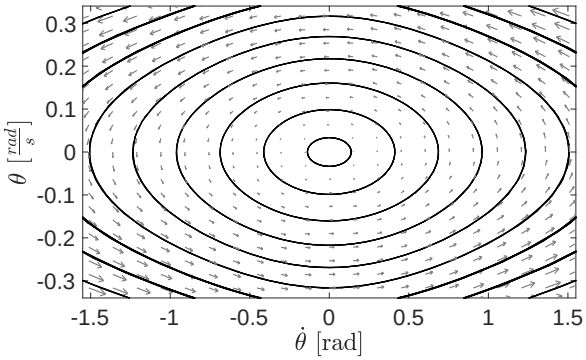

Figure 8. Graphical representation of the modal dynamics (45) of the SLIP system of Eq. (41), for $\kappa_1=20\frac{1}{s^2}$, $\kappa_2=60\frac{1}{s^2}$, $g=9.81\frac{\mathrm{m}}{\mathrm{s}^2}$, $r_0=1$m. Solid lines are examples of trajectories. Arrows represent the tangent force field.

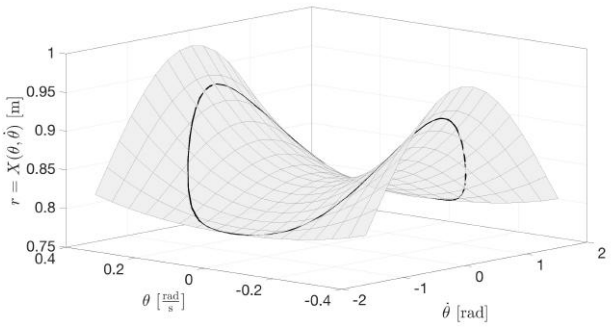

(a)

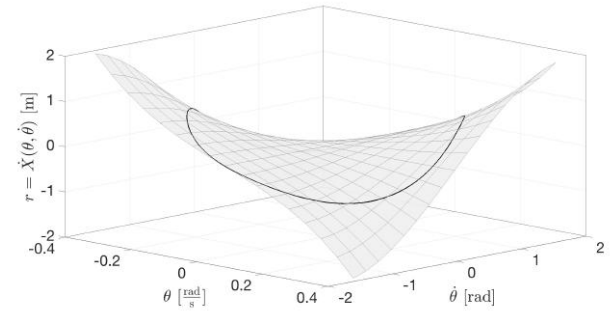

(b)

Figure 9. Graphical representation of the modal invariant manifold (44) of the SLIP (41), for $\kappa_1=20\frac{1}{s^2}$, $\kappa_2=60\frac{1}{s^2}$, $g=9.81\frac{\mathrm{m}}{\mathrm{s}^2}$, $r_0=1$m. The solid line is the trajectory corresponding to the initial condition $\theta=0$ and $\dot\theta=\frac{\pi}{2}\frac{\mathrm{rad}}{\mathrm{s}}$.

Thus the second condition of Theorem 1 can be applied. We consider here a pure damping feedback on the slave variable r, resulting in the following control law

$$\begin{cases} \tau_1= & -2\frac{\dot X(\theta,\dot\theta)r-X(\theta,\dot\theta)\dot r}{X(\theta,\dot\theta)r}\dot\theta+g\frac{r-X(\theta,\dot\theta)}{X(\theta,\dot\theta)r}\sin(\theta) \\ & -\kappa_1\frac{r^2-X(\theta,\dot\theta)^2}{X(\theta,\dot\theta)^2r^2}\theta \\ \tau_2= & \kappa_\mathrm{d}(\dot r-\dot X(\theta,\dot\theta))\,, \end{cases} \tag{47}$$

which, from (19), stabilizes the manifold if

$$\kappa_2>\dot\theta^2\,,\quad \kappa_\mathrm{d}>\frac{2\dot\theta\ddot\theta}{\dot\theta^2-\kappa_2}\,, \tag{48}$$

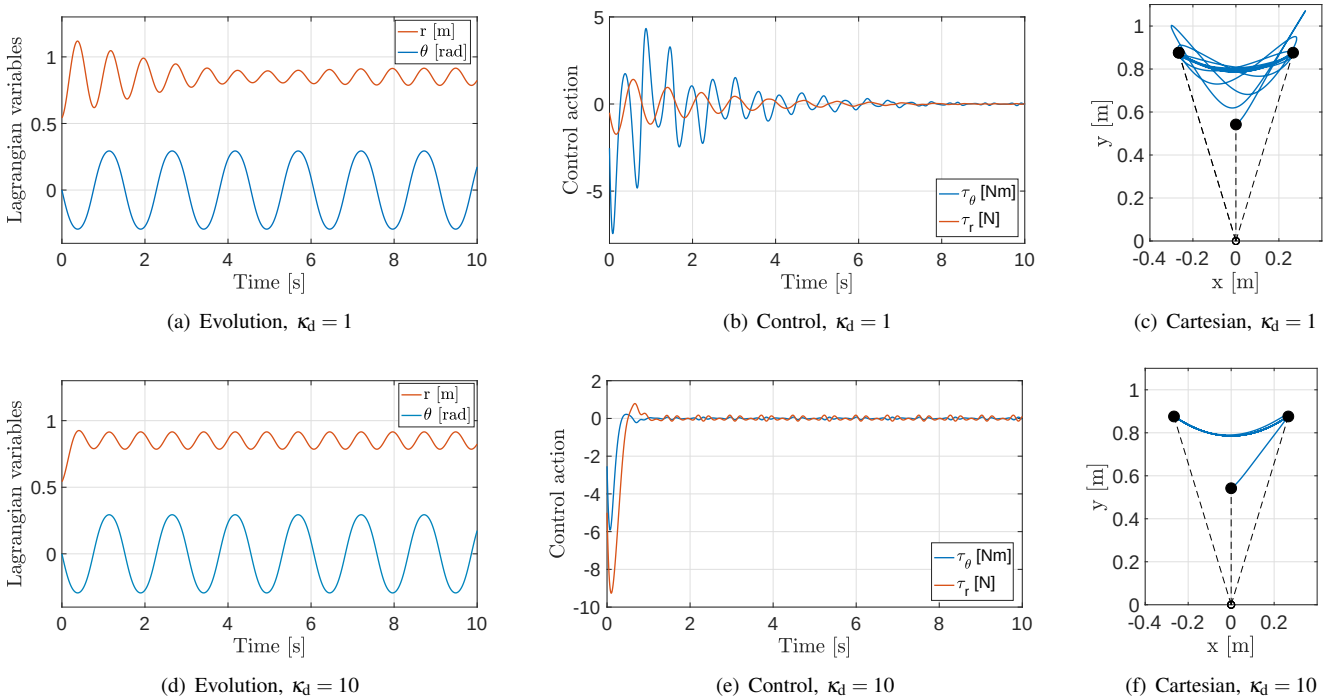

(a) Evolution, $\kappa_d = 1$ (b) Control, $\kappa_d = 1$ (c) Cartesian, $\kappa_d = 1$

(d) Evolution, $\kappa_d = 10$ (e) Control, $\kappa_d = 10$ (f) Cartesian, $\kappa_d = 10$

Figure 10. Inverted elastic pendulum (41) controlled through (17), with $\kappa_d = 1$ (a,b,c), $\kappa_d = 10$ (d,e,f). The considered physical parameters are $\kappa_1 = 20\frac{1}{s^2}$, $\kappa_2 = 60\frac{1}{s^2}$, $g = 9.81\frac{m}{s^2}$, $r_0 = 1$m. The selected initial condition is $\theta = 0$, $\dot{\theta} = \frac{7}{16}\pi\frac{rad}{s}$, $r \simeq 0.54$m, $\dot{r} = 0.5\frac{m}{s}$. Note that for these values the system is outside the invariant manifold, indeed $r(0) - X(\theta(0), \dot{\theta}(0)) \simeq -\frac{1}{4}$m and $\dot{r}(0) - \dot{X}(\theta(0), \dot{\theta}(0)) = -0.5\frac{m}{s}$. Panels (a,d) present the time evolution of the Lagrangian variables θ and r. Panels (b,e) show the control action generated by the controller. Panels (c,f) present the evolution of the mass in Cartesian space.

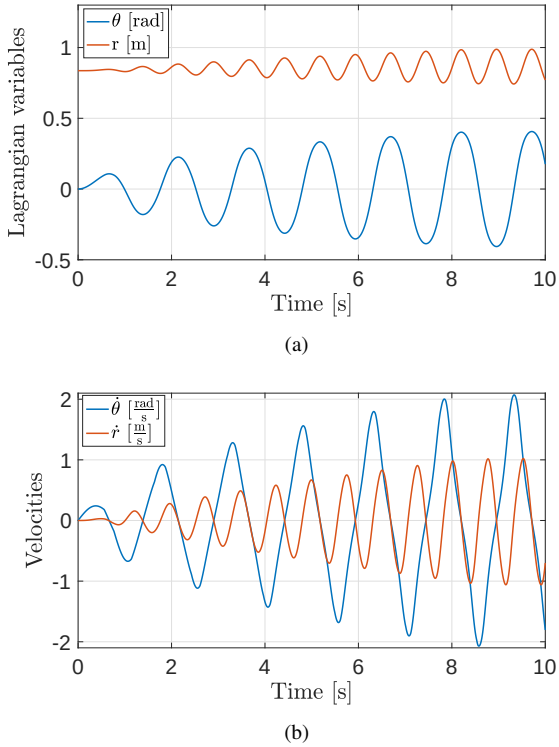

(a)

(b)

Figure 11. Evolution of inverted elastic pendulum (41) controlled through (34), with $\kappa_d = 10\frac{Ns}{m}$, $E^- = 21$J, $E^+ = 22$J, $x^- = -\frac{\pi}{32}$, $x^+ = +\frac{\pi}{32}$, $\gamma = 1$N. The system starts from the equilibrium $r = r_0 - \frac{g}{\kappa_1}$, $\theta = 0$. The controller successfully increases the system oscillations, while maintaining the two degrees of freedom synchronized (i.e. on the modal manifold). This is particularly evident in panel (b).

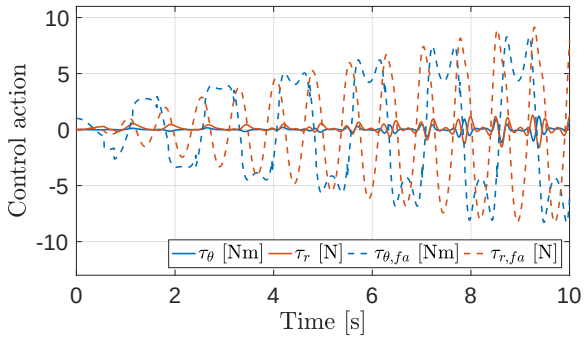

Figure 12. The control actions generated by (34) while controlling (41) are presented in solid line. The consider parameters are $\kappa_d = 10\frac{Ns}{m}$, $E^- = 21$J, $E^+ = 22$J, $x^- = -\frac{\pi}{32}$, $x^+ = +\frac{\pi}{32}$, $\gamma = 1$N, and initial condition $r = r_0 - \frac{g}{\kappa_1}$, $\theta = 0$. The dashed lines indicate the corresponding actions that would have been needed to implement the same behavior in a rigid system.

where $\ddot{\theta}$ is defined by (45). Note that all the terms in (47) are polynomial, except for $\sin(\theta)$. This makes the control evaluation relatively fast, and easily implementable in real time.

Fig. 10 presents the evolution of the system (41) controlled by (47), for two different choices of κ_d: a low gain $\kappa_d = 1\frac{Ns}{m}$, and an higher one $\kappa_d = 10\frac{Ns}{m}$. The initial condition is $\theta = 0$, $\dot{\theta} = \frac{7}{16}\pi$, $r = X(0, \frac{7}{16}\pi) - \frac{1}{4}$m $\simeq 0.54$m, $\dot{r} = \dot{X}(0, \frac{7}{16}\pi) - 0.5\frac{m}{s} = 0.5\frac{m}{s}$. In both cases the robot converges to a stable running-like oscillation. Panels (a,d) show the time evolutions. In the less damped case the r variable converges

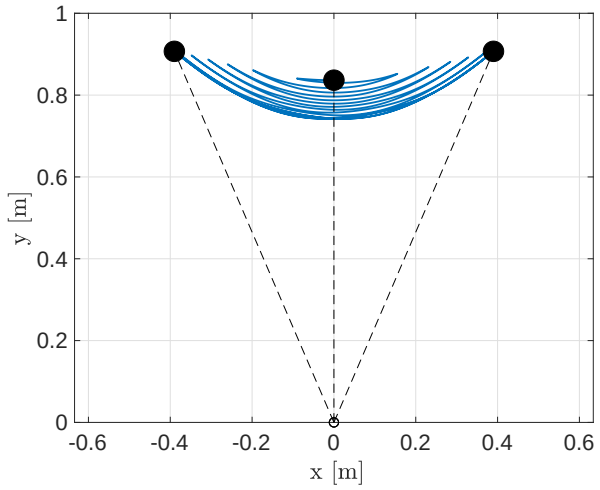

Figure 13. Cartesian evolution of inverted elastic pendulum (41) controlled through (34), with $\kappa_d = 10$, $E^- = 21$J, $E^+ = 22$J, $x^- = -\frac{\pi}{32}$, $x^+ = +\frac{\pi}{32}$, $\gamma = 1$N. The system starts from the equilibrium $r = r_0 - \frac{g}{\kappa_1}$, $\theta = 0$. Note that due to the particular choice of κ_1 and κ_2 trajectories are convex for all the simulated evolutions.

more slowly and with an overshoot. Looking to the control actions (b,e), this translates into a much more complex action of the decoupling controller τ_θ. Note that in both cases the control action converges to zero, i.e. the robot evolves on the manifold following autonomous trajectories. Panels (c,f) show the trajectory of the center of mass in the Cartesian space. In (c) a much more dynamic transient can be observed.

Fig. 11 presents the time evolutions of system (41) controlled through (34). Note that the system is conservative, and the energy

$$E(\theta,\dot\theta,r,\dot r) = \frac{1}{2}(r^2\dot\theta^2+\dot r^2) + \frac{1}{2}(\kappa_1\theta^2+\kappa_2(r-r_0)^2) + g\,(r\cos(\theta)) \tag{49}$$

has closed level curves, thus fulfilling the hypotheses of Theorem 2. We considered $E^- = 21$J, $E^+ = 22$J, $x^- = -\frac{\pi}{32}$, $x^+ = +\frac{\pi}{32}$, $\gamma = 1$N. The system starts at the equilibrium, i.e. $\theta = 0$, $r = r_0 - \frac{g}{\kappa_2} \simeq 0.84\,m$, $\dot\theta = 0$, $\dot r = 0$. The orbit excitation controller perturbs the system putting it in oscillation. The system reaches the desired level of energy at about 9s. Note that thanks to the stabilizing controller, evolutions remain synchronized during the whole excitation phase despite the perturbations. This is particularly evident from the zero-crossings of the velocities, Fig. 11 panel (b).

The same figure also highlights a key characteristic of the considered mode: the frequency of oscillation of θ is half of the frequency of oscillation of r. This is a purely nonlinear behavior, made possible by the fact that the parametrization of the manifold X decreases in one direction and increases in the other (see Fig.s 9(a) and 9(b)).

For the same simulation, Fig. 12 presents a comparison between the control actions exerted by the proposed controller (τ_θ and τ_r), and the ones that would have been necessary to regulate an equivalent rigid robot along the same trajectory ($\tau_{\theta,\mathrm{fa}}$ and $\tau_{r,\mathrm{fa}}$). For all the evolution the soft robot controlled through the proposed controller visibly outperform the rigid counterpart. The forces are in the worst case around one order of magnitude less than the control actions needed to a non elastic version of the robot to implement the same trajectory, as shown by Fig. 12(b). Finally, Fig. 13 presents the Cartesian evolution of the center of mass.

VI. Experimental Results: Oscillatory Control of a Segmented Leg

As a first experimental validation of the proposed strategy, we consider the soft segmented leg in Fig. 14. We are interested here in generating swing oscillations of its center of mass, in analogy to what was obtained in simulation. The segmented leg is composed by two links of the same length a, considered here massless, and a main body, with mass m. The leg is mechanically constrained to evolve on the sagittal plane, and the main body to remain vertical. We hypothesize infinite friction between the foot and the environment. Thus the configuration of the robot can be described by the two angles q_1 and q_2 in Fig. 14.

We consider the following change of coordinates,

$$\begin{aligned}\theta &= \frac{q_1+q_2}{2}\\ r &= a\sqrt{2(1+\cos(q_1-q_2))},\end{aligned} \tag{50}$$

where θ and r are the polar coordinates of the center of mass w.r.t. the foot position. The resulting dynamics has the SLIP-like form (see [30] for the detailed derivation)

$$\begin{cases}\ddot\theta = -2\frac{\dot r}{r}\dot\theta + \frac{g}{r}\sin(\theta) - \frac{2\kappa\theta}{r^2} + \tau_\theta\\ \ddot r = +r\dot\theta^2 - g\cos(\theta) - \kappa\frac{1}{\sqrt{4a^2-r^2}}(\rho(r)-\rho(r_0)) + \tau_\mathrm{r}\end{cases} \tag{51}$$

where $\rho(r) = \arccos(1-\frac{r^2}{2a^2})$, κ is the stiffness of both springs, τ_θ and τ_r are the control actions, and the other terms are as in (41). The maps $X(\theta,\dot\theta)$ and $\dot X(\theta,\dot\theta)$ can be evaluated as in the SLIP case (see Sec. V-B), and they are not reported here for the sake of space.

Note that the physical system presents several non ideal effects making its control challenging, as e.g. actuator dynamics, contact with the ground, non zero weight of the legs, inexact identification of system parameters, neglected friction effects. Furthermore, the angular velocity $\dot\theta$ could not be directly measured, and it was instead estimated through a simple high pass filter.

Though it is beyond the scope of this paper to investigate robustness analytically, we empirically test it here with this example, where we do not assume any knowledge of the dynamic form in the decoupling control. We instead consider only the two main ingredients of the proposed control strategy (34), i.e. an excitatory action in the direction of the master variable θ, and a damping action along the slave direction r

$$\tau(\theta,\dot\theta) = \begin{bmatrix}\bar\tau_1(\theta,\dot\theta)\\ 10\,(\dot r - \dot X(\theta,\dot\theta))\end{bmatrix}, \tag{52}$$

where $\bar\tau_1$ is as in (35). Empirically we considered a high gain for the damping controller, since in the simulative case this

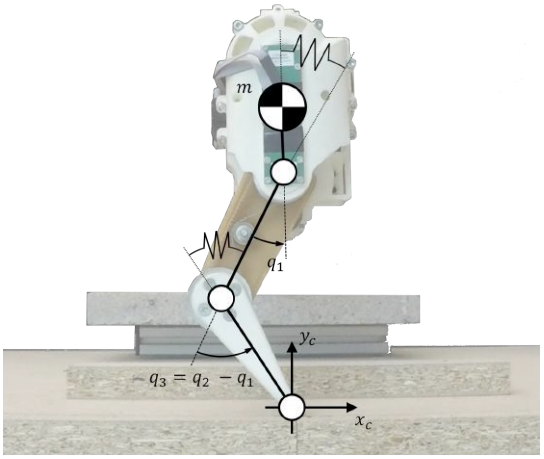

Figure 14. Experimental setup: a 2-DoF (the upper part is constrained to stay vertical) segmented leg. A sketch of the robot with main quantities highlighted is superimposed.

translated into a small authority of the decoupling controller neglected here.

As in simulation, we consider the target energy level $E^- = 21$J, $E^+ = 22$J. We performed experiments for five different values of the orbit excitation gain α in $\bar{\tau}_1$: 0.2Nm, 0.3Nm, 0.5Nm, 0.7Nm, 0.9Nm. Due to friction, the desired level of energy could not be reached. Instead energy injected through $\bar{\tau}_1$ is compensated by the dissipation and a different equilibrium is reached for each value of α. Fig. 15 presents the photo-sequences of a single oscillation for two of the considered gains. Fig. 16 presents the evolution of θ and r for $\alpha = 0.5$Nm. Control action is turned on at 0s, and it takes about 2s to bring the system on a stable oscillation. It is worth noticing that the resulting nonlinear oscillation (θ, r) is actually very close to the ideal one $(\theta, X(\theta, \dot{\theta}))$, as evidenced by Panel (b) of the same figure.

Fig. 17 shows the center of mass' evolutions in Cartesian coordinates, for all the considered gains and for a period of 15s. Note that the bigger is the gain, the larger are the oscillations, i.e. the higher is the energy level reached. The resulting oscillations are slightly concave, and highly repeatable.

These results suggest that the proposed strategy can be used to excite the normal modes of soft robots, generating stable and repeatable nonlinear oscillations also in the presence of many unideal behaviors in the controlled system.

Fig. 18 illustrates the resulting evolutions superimposed to the ideal modal manifold, i.e. to the surface $r = X(\theta, \dot{\theta})$. The matching is good, with larger discrepancies for high speeds and positive values of θ. The asymmetry of behavior w.r.t. to θ was already evident in Fig. 16, and it is probably due to the effect of leg dynamics, which is neglected in (51). The error observed for large velocities is instead probably due to the persistent excitation (as theoretically discussed in Sec. IV-C), and to the imperfect knowledge of $\dot{\theta}$. Future work will be devoted to more in-depth analysis of the theoretical implications of these aspects.

Finally, the algorithm was preliminarily tested on a quadruped built using four of the above discussed soft segmented legs. The proposed control strategy is able to excite stable natural oscillations also in this more complex system, as shown in Fig. 19. Future work will be devoted to the exploitation of such oscillations in performing efficient locomotion patterns.

VII. Conclusions

Soft Robots are robotic systems in which elastic elements are purposefully introduced in the mechanical structure. It is thus intuitively clear that soft robots should be able to perform oscillatory tasks with good efficiency. We formalized this intuition in the linear case in Sec. II. However, the nonlinearities of the robot dynamics make the problem of studying and generating oscillations non-trivial. Classical techniques can regulate the system on a specific trajectory or limit cycle by a partial or complete cancellation of the dynamics, thus defeating the purpose of introducing springs. In this work we took inspiration from the natural world and from nonlinear dynamical system theory, proposing to generate very efficient oscillations in soft robots by regulating the system on a nonlinear extension of a linear eigenspace. This way the natural dynamics of the system is fully exploited. After a brief survey about the nonlinear normal mode theory, we moved to the mode stabilization in the nonlinear case. We also considered the problem of exciting a specific set of trajectories on the manifold. We then discussed the analysis problem, proposing an approximated analytic solution for the SLIP model. Simulations were presented to show the effectiveness of the method. Finally, leveraging on insights gained from simulations, an empirical simplification of the proposed controller is used to experimentally induce nonlinear oscillations in a segmented leg. In addition to showing the practical feasibility and robustness of the method, experiments served to understand its main practical limitations, which we briefly discussed at the end of the same section.

Many are the aspects of this work that will require further investigation in the future. For what concerns the control part, future work will be devoted to better understanding the role of the decoupling controller, and to the possibility of generating persistent oscillatory actions without sensibly changing the manifold shape. e.g. by exciting nonlinear resonances (as it happens in the linear case). Regarding the analysis problem, application to multi-DoF soft robotics systems calls for the development of novel tools and techniques for NNM analytical derivation. Finally, from an experimental point of view our work will focus on implementing stable natural oscillations in more complex systems and meaningful tasks, as the execution of locomotion gates with legged robots, oscillatory pick and place with multi-DoF soft arms, etc.

Appendix A

We present in this section the proof of Proposition 1.

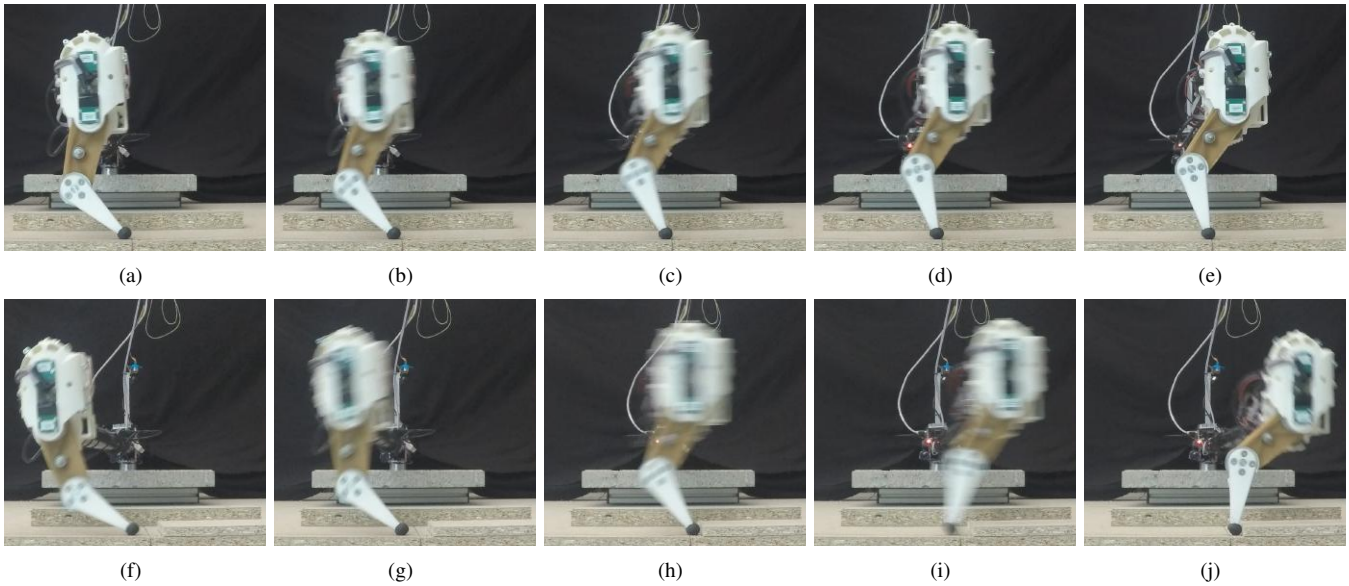

Figure 15. Photo-sequences of nonlinear oscillations induced by the proposed algorithm on a segmented soft leg. Panels (a-e) present one oscillation for $\alpha = 0.3$Nm, while panels (f-j) show the case of $\alpha = 0.9$Nm.

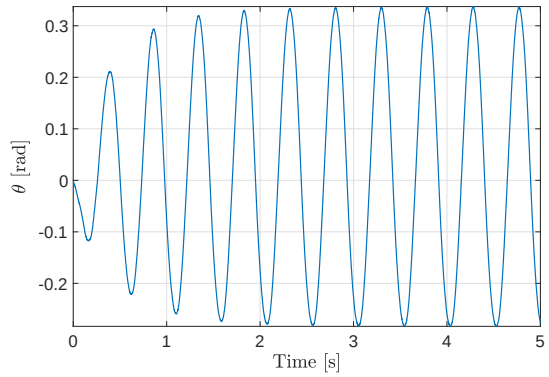

(a)

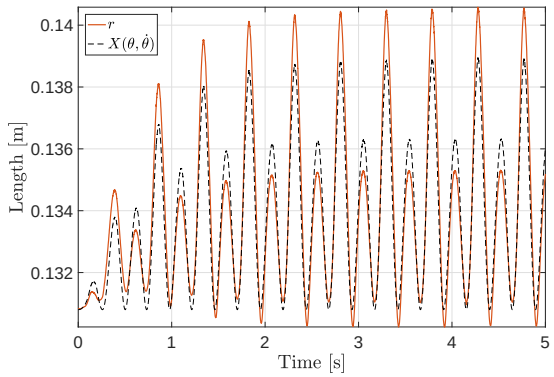

(b)

Figure 16. Experimental evolutions of master variable θ and slave variable r, for $\alpha = 0.5$Nm. After an initial transient in which the algorithm injects energy, the segmented leg starts to evolve according to a stable nonlinear oscillation. Panel (b) also presents the ideal evolution on the manifold $X(\theta, \dot{\theta})$ of the slave variable r for the measured evolution of θ.

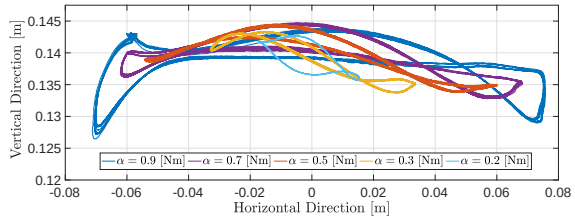

Figure 17. Experimental trajectories in Cartesian coordinates of the segmented leg's center of mass controlled through (52), with different values of the energy injection gain α. Stable oscillations result for all the considered gains.

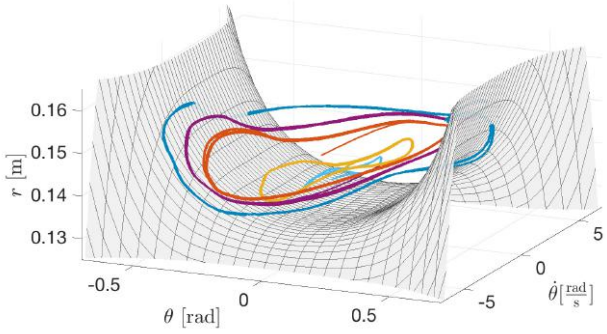

Figure 18. Experimental evolutions represented in the space $(\theta, \dot{\theta}, r)$, obtained for several choices of the gain α and 15s of oscillations. We also superimpose the ideal modal manifold $r = X(\theta, \dot{\theta})$. The matching is good for all the considered gains, despite the many unideal characteristics of the system.

Proof. Lets express (1) in state form by considering the state vector $[p^{\mathrm{T}} \ v^{\mathrm{T}}]^{\mathrm{T}} = [x^{\mathrm{T}} \ \dot{x}^{\mathrm{T}}]^{\mathrm{T}}$

$$\begin{bmatrix} \dot{p} \\ \dot{v} \end{bmatrix} = \begin{bmatrix} 0 & \mathrm{I} \\ -M^{-1}K & 0 \end{bmatrix} \begin{bmatrix} p \\ v \end{bmatrix} + \begin{bmatrix} 0 \\ M^{-1}\tau \end{bmatrix} . \tag{53}$$

Consider the orthonormal matrix $V \in \mathbb{R}^{n \times n}$, such that $J = V^{\mathrm{T}} K V$ is in Jordan form. By considering the following change

(a) (b) (c) (d) (e)

Figure 19. Photo-sequence of nonlinear oscillatory behavior induced on a soft quadruped by the proposed algorithm. While preliminary, this experiment shows the ability of the strategy to deal with more complex systems.

of coordinates,

$$\begin{bmatrix}\pi\\ \upsilon\end{bmatrix} = \begin{bmatrix}V & 0\\ 0 & V\end{bmatrix}\begin{bmatrix}p\\ v\end{bmatrix} \tag{54}$$

the dynamics (53) becomes

$$\begin{bmatrix}\dot{\pi}\\ \dot{\upsilon}\end{bmatrix} = \begin{bmatrix}0 & \mathrm{I}\\ -J & 0\end{bmatrix}\begin{bmatrix}\pi\\ \upsilon\end{bmatrix} + \begin{bmatrix}0\\ f\end{bmatrix} \tag{55}$$

where $f = V^{\mathrm{T}}M^{-1}\tau$. This is equivalent to a set of decoupled systems in the form

$$\begin{bmatrix}\pi_i\\ \upsilon_i\end{bmatrix} = \begin{bmatrix}0 & I_{m_i\times m_i}\\ -J_i & 0\end{bmatrix}\begin{bmatrix}\pi_i\\ \upsilon_i\end{bmatrix} + \begin{bmatrix}0\\ f_i\end{bmatrix}, \tag{56}$$

where $\pi_i, \upsilon_i, f_i \in \mathbb{R}^{m_i}$ are elements of π, υ, f related to the $i-$th eigenspace. J_i is the $i-$th diagonal block of J.

Consider now the following relationship

$$K^{\frac{1}{2}}(M^{-1}K)K^{-\frac{1}{2}} = K^{\frac{1}{2}}M^{-1}K^{\frac{1}{2}} = (K^{\frac{1}{2}}M^{-1}K^{\frac{1}{2}})^{\mathrm{T}} \tag{57}$$

where we exploited the hypothesis $K \succ 0$ to define $K^{\frac{1}{2}}$, and the symmetry of both K and M in the second step. Eq. (57) tells us that $M^{-1}K$ is similar to a symmetric matrix. Thus all its eigenvalues are real.

Note also that $\forall v \in \mathbb{R}^{m_i}$

$$v^{\mathrm{T}}K^{\frac{1}{2}\mathrm{T}}M^{-1}K^{\frac{1}{2}}v = (K^{\frac{1}{2}}v)^{\mathrm{T}}M^{-1}(K^{\frac{1}{2}}v) > 0\,, \tag{58}$$

where in the last step we exploited that $M \succ 0 \Rightarrow M^{-1} \succ 0$. Thus, $M^{-1}K$ is similar to a positive and symmetric matrix, and therefore all its eigenvalues are also positive.

This implies that J_i has the form

$$J_i = \begin{bmatrix}\lambda_i & 1 & 0 & \cdots & 0\\ 0 & \lambda_i & 1 & \cdots & 0\\ \vdots & \vdots & \vdots & \ddots & \vdots\\ 0 & 0 & 0 & \lambda_i & 1\\ 0 & 0 & 0 & 0 & \lambda_i\end{bmatrix}, \tag{59}$$

with $\lambda_i > 0$. This is in turn implies that through simple permutations the system (56) can be expressed as a series of m_i linear oscillators

$$\begin{bmatrix}\pi_{i,j}\\ \upsilon_{i,j}\end{bmatrix} = \begin{bmatrix}0 & 1\\ -\lambda_i & 0\end{bmatrix}\begin{bmatrix}\pi_{i,j}\\ \upsilon_{i,j}\end{bmatrix} + \begin{bmatrix}0\\ f_{i,j}\end{bmatrix} - \begin{bmatrix}0\\ \pi_{i,j-1}\end{bmatrix}, \tag{60}$$

where $\pi_{i,j}, \upsilon_{i,j}, f_{i,j} \in \mathbb{R}$ are the $j-$th elements of $\pi_i, \upsilon_i, f_i \in \mathbb{R}^{m_i}$. Note that series of linear systems are stable if each subsystem is stable. Thus to stabilize (56) it is sufficient to damp each oscillator separately. At this end we can use

$$f_i = -\beta\,\upsilon_i\,, \tag{61}$$

where $\beta \in \mathbb{R}^+$ is a strictly positive constant.

So, to make attractive the eigenspace associated to the first eigenvector it will be sufficient to regulate at 0 the dynamics expressed on all the other eigenspaces. This can be done by applying (61) for all $i \neq 1$

$$f = -\beta\begin{bmatrix}0_{m_1\times m_1} & 0_{m_1\times n-m_1}\\ 0_{n-m_1\times m_1} & \mathrm{I}_{n-m_1\times n-m_1}\end{bmatrix}\upsilon\,. \tag{62}$$

In the original coordinates (62) is

$$\tau = -\beta MV\begin{bmatrix}0_{m_1\times m_1} & 0_{m_1\times n-m_1}\\ 0_{n-m_1\times m_1} & \mathrm{I}_{n-m_1\times n-m_1}\end{bmatrix}V^{\mathrm{T}}\dot{x}. \tag{63}$$

□

Appendix B

In this appendix we propose two lemmas about the stability of linear time variant mechanical system, which are instrumental to the proof of Theorem 1. Lets consider the system

$$\begin{bmatrix}\dot{p}\\ \dot{v}\end{bmatrix} = \begin{bmatrix}0 & \mathrm{I}\\ -K(t) & -D(t)\end{bmatrix}\begin{bmatrix}p\\ v\end{bmatrix}, \tag{64}$$

where $p \in \mathbb{R}^n$ is the system configuration space, $v \in \mathbb{R}^n$ are the velocities. $K(t) \in \mathbb{R}^{n\times n}$ and $D(t) \in \mathbb{R}^{n\times n}$ are respectively the time-varying stiffness and damping.

Lemma 1. *A $\delta < \infty$ always exists such that if $||\dot{K}(t)|| < \delta$, $||\dot{D}(t)|| < \delta$, $\rho(K(t)) > 0$, and $\rho(D(t)) > 0$, then* (64) *is stable.*

Proof. We prove here the thesis in the case of Frobenious norm. This is without loss of generality since any other standard matrix norm can be upper and lower bounded by the Frobenious norm [56].

Classic results [57] assure that always exists a $\gamma \in \mathbb{R}^+$ such that if

$$\left|\left|\frac{\mathrm{d}}{\mathrm{d}t}\begin{bmatrix}0 & \mathrm{I}\\ -K(t) & -D(t)\end{bmatrix}\right|\right|_{\mathrm{F}} < \gamma \tag{65}$$

and

$$\rho\left(\begin{bmatrix}0 & \mathrm{I}\\ -K(t) & -D(t)\end{bmatrix}\right) < 0 \quad \forall t\,, \tag{66}$$

then (64) is stable.

The first condition is assured by considering $\gamma = \sqrt{2}\delta$

$$\begin{aligned}\left|\left|\frac{\mathrm{d}}{\mathrm{d}t}\begin{bmatrix}0 & \mathrm{I}\\ -K(t) & -D(t)\end{bmatrix}\right|\right|^2_{\mathrm{F}} &= \left|\left|\begin{bmatrix}0 & 0\\ -\dot{K}(t) & -\dot{D}(t)\end{bmatrix}\right|\right|^2_{\mathrm{F}}\\ &= ||\dot{K}(t)||^2_{\mathrm{F}} + ||\dot{D}(t)||^2_{\mathrm{F}}\\ &\leq 2\,\delta^2 = \gamma^2\,,\end{aligned} \tag{67}$$

which leads to (66) by extracting the square root.

It is worth noticing that condition (66) is equivalent to considering the stability of all the possible time invariant

systems obtained by fixing the time in the dynamic matrix. Thus we can prove condition (66) by considering that a sufficient condition for the stability of a linear mechanical system is that its stiffness and damping matrices are both positive definite. This is assured by the hypotheses $\rho(K(t)) > 0$, and $\rho(D(t)) > 0$. □

Lemma 2. *If $M(t) \in \mathbb{R}^{n\times n}$ exists such that $M^T K M$ and $M^T D M$ are both diagonal $\forall t$, and if*

$$\lambda_i(K(t)) > 0, \quad \lambda_i(D(t)) > -\frac{\lambda_i(\dot{K}(t))}{\lambda_i(K(t))} \quad \forall t \tag{68}$$

where $\lambda_i(\cdot)$ extracts the eigenvalue corresponding to the $i-th$ column of $M(t)$, then (64) *is stable.*

Proof. By considering the following change of coordinates,

$$\begin{bmatrix}\pi\\ \upsilon\end{bmatrix} = \begin{bmatrix}M(t) & 0\\ 0 & M(t)\end{bmatrix}\begin{bmatrix}p\\ v\end{bmatrix}$$

the dynamics becomes equivalent to a set of decoupled undimensional time variant oscillators

$$\begin{bmatrix}\dot{\pi}_i\\ \dot{\upsilon}_i\end{bmatrix} = \begin{bmatrix}0 & 1\\ -\lambda_i(K(t)) & -\lambda_i(D(t))\end{bmatrix}\begin{bmatrix}\pi_i\\ \upsilon_i\end{bmatrix}.$$

The stability of such system under the bounds (68) can be proven using the Lyapunov candidate

$$V(\pi_i, \upsilon_i, t) = \pi_i^2 + \frac{\upsilon_i^2}{\lambda_i(K(t))},$$

and the Barbalat lemma. For the sake of conciseness we do not report here the whole derivation, that can be found in [58]. □

Appendix C

We report in the following the 16 algebraic equations resulting from the evaluation of Eq. (9) for the system (41)

$$\begin{cases}
b_{10} - a_{13}\,d_1 + a_4\,d_6 = 0\\
b_{13} - 4\,a_{10} - 2\,a_{12}\,d_1 + a_4\,d_5 + 2\,a_5\,d_6 = 0\\
b_{12} - 3\,a_{13} - 3\,a_{11}\,d_1 + 2\,a_5\,d_5 + a_4\,d_7 = 0\\
b_3 - a_4\,d_1 = 0\\
b_{11} - 2\,a_{12} - 4\,a_{14}\,d_1 + 2\,a_5\,d_7 + 2\,a_4\,b_5\,d_3 = 0\\
b_4 - 2\,a_3 - 2\,a_5\,d_1 = 0\\
b_{14} - a_{11} + 4\,a_5\,b_5\,d_3 = 0\\
b_5 - a_4 = 0\\
b_4\,d_6 - b_{13}\,d_1 - a_{10}\,\kappa_2 = 0\\
b_4\,d_5 - a_{13}\,\kappa_2 - 2\,b_{12}\,d_1 - 4\,b_{10} + 2\,b_5\,d_6 = 0\\
a_3 - 3\,b_{13} - a_{12}\,\kappa_2 - 3\,b_{11}\,d_1 + 2\,b_5\,d_5 + b_4\,d_7 = 0\\
g - 2\,a_3\,\kappa_2 - 2\,b_4\,d_1 = 0\\
a_4 - 2\,b_{12} - a_{11}\,\kappa_2 - 4\,b_{14}\,d_1 + 2\,b_5\,d_7 + 2\,b_4\,b_5\,d_3 = 0\\
2\,b_3 + a_4\,\kappa_2 + 2\,b_5\,d_1 = 0\\
a_5 - b_{11} - a_{14}\,\kappa_2 + 4\,{b_5}^2\,d_3 = 0\\
r_0 - b_4 - a_5\,\kappa_2 - \frac{g}{\kappa_2} = 0
\end{cases} \tag{69}$$

where

$$\begin{cases}
d_1 = g\left(\frac{1}{r_0} + \frac{g}{\kappa_2\,{r_0}^2} + \frac{g^2}{{\kappa_2}^2\,{r_0}^3}\right) - \kappa_1\left(\frac{1}{{r_0}^2} + \frac{2\,g}{\kappa_2\,{r_0}^3} + \frac{3\,g^2}{{\kappa_2}^2\,{r_0}^4}\right)\\
d_2 = \frac{1}{{r_0}^2} + \frac{2\,g}{\kappa_2\,{r_0}^3}\\
d_3 = \frac{1}{r_0} + \frac{g}{\kappa_2\,{r_0}^2}\\
d_4 = \frac{2}{{r_0}^3} + \frac{6\,g}{\kappa_2\,{r_0}^4}\\
d_5 = 2\,b_3\,d_3 + g\,a_4\,d_2 - \kappa_1\,a_4\,d_4\\
d_6 = g\,a_3\,d_2 - \kappa_1\,a_3\,d_4 + \frac{g}{6\,r_0}\\
d_7 = 2\,b_4\,d_3 + g\,a_5\,d_2 - \kappa_1\,a_5\,d_4
\end{cases} \tag{70}$$

Appendix D

We present here the coefficients of the manifold parametrization $X(\theta,\dot{\theta})$ and $\dot{X}(\theta,\dot{\theta})$ derived in Sec. V in the form described by (44), when $r_0 = 1\text{m}$ and $g = 9.81\,\frac{\text{Nm}}{\text{s}^2}$

$$a_i(\kappa_1,\kappa_2) = -\frac{\alpha_i(\kappa_1,\kappa_2)}{\gamma_i(\kappa_1,\kappa_2)} \tag{71}$$

$$\alpha_3 = 5\left(-400\,{d_1}^2\,\kappa_2 + 3.9\,10^3\,{d_1}^2 + 2\,10^3\,d_1\,\kappa_2 + 999\,{\kappa_2}^2\right) \tag{72}$$

$$\gamma_3 = 10^3\,{\kappa_2}^2\,(4\,d_1 + \kappa_2) \tag{73}$$

$$\alpha_5 = -20\,d_1 + 20\,\kappa_2 - 2\,d_1\,\kappa_2 - {\kappa_2}^2 \tag{74}$$

$$\gamma_5 = {\kappa_2}^2\,(4\,d_1 + \kappa_2) \tag{75}$$

$$\begin{aligned}
\alpha_{12} &= 1.2\,10^5\,{d_1}^3\,d_2 - 2.7\,10^3\,d_1\,{\kappa_2}^3 + 144\,d_1\,{\kappa_2}^4\\
&- 2.6\,10^4\,d_2\,{\kappa_2}^3 + 2.5\,10^3\,{d_1}^4\,\kappa_2 + 788\,d_2\,{\kappa_2}^4 + 399\,d_3\,{\kappa_2}^4\\
&- 788\,{\kappa_2}^4 + 29\,{\kappa_2}^5 + 1.5\,10^3\,{d_1}^2\,{\kappa_2}^2 + 688\,{d_1}^2\,{\kappa_2}^3 + 3\,10^3\,{d_1}^3\,{\kappa_2}^2\\
&- 28\,{d_1}^2\,{\kappa_2}^4 - 199\,{d_1}^3\,{\kappa_2}^3 - 277\,{d_1}^4\,{\kappa_2}^2 - 9.2\,10^3\,{d_1}^2\,d_2\,{\kappa_2}^2\\
&+ 488\,{d_1}^2\,d_2\,{\kappa_2}^3 + 1.3\,10^3\,{d_1}^3\,d_2\,{\kappa_2}^2 - 633\,{d_1}^2\,d_3\,{\kappa_2}^3\\
&- 3.1\,10^3\,{d_1}^3\,d_3\,{\kappa_2}^2 + 64\,{d_1}^2\,d_3\,{\kappa_2}^4 + 177\,{d_1}^3\,d_3\,{\kappa_2}^3\\
&+ 4.5\,10^4\,{d_1}^2\,d_2\,\kappa_2 - 4.6\,10^3\,d_1\,d_2\,{\kappa_2}^3 - 2.5\,10^4\,{d_1}^3\,d_2\,\kappa_2\\
&+ 177\,d_1\,d_2\,{\kappa_2}^4 - 4.6\,10^3\,d_1\,d_3\,{\kappa_2}^3 + 1.5\,10^4\,{d_1}^3\,d_3\,\kappa_2\\
&- 1.2\,10^4\,{d_1}^3\,d_4\,\kappa_1 + 400\,d_1\,d_3\,{\kappa_2}^4 + 2.7\,10^3\,d_4\,\kappa_1\,{\kappa_2}^3\\
&- 78\,d_4\,\kappa_1\,{\kappa_2}^4 - 4.6\,10^3\,{d_1}^2\,d_4\,\kappa_1\,\kappa_2 + 488\,d_1\,d_4\,\kappa_1\,{\kappa_2}^3\\
&+ 2.5\,10^3\,{d_1}^3\,d_4\,\kappa_1\,\kappa_2 - 16\,d_1\,d_4\,\kappa_1\,{\kappa_2}^4 + 944\,{d_1}^2\,d_4\,\kappa_1\,{\kappa_2}^2\\
&- 48\,{d_1}^2\,d_4\,\kappa_1\,{\kappa_2}^3 - 133\,{d_1}^3\,d_4\,\kappa_1\,{\kappa_2}^2
\end{aligned} \tag{76}$$

$$\gamma_{12} = 2\,{\kappa_2}^4\,(4\,d_1 + \kappa_2)^2\,(16\,d_1 + \kappa_2) \tag{77}$$

$$\begin{aligned}
&\alpha_{14}(\kappa_1,\kappa_2) = 2\,10^5\, {d_1}^2 d_2 \\
&+ 9.2\,10^3\, {d_1}^3 d_3 + 2.7\,10^3\, d_1\, {\kappa_2}^2 - 1.5\,10^3\, {d_1}^2\, \kappa_2 \\
&- 566\, d_1\, {\kappa_2}^3 + 3.4\,10^4\, d_2\, {\kappa_2}^2 - 4.2\,10^3\, {d_1}^3\, \kappa_2 + 22\, d_1\, {\kappa_2}^4 \\
&- 1.5\,10^3\, d_2\, {\kappa_2}^3 + 277\, {d_1}^4\, \kappa_2 + 20\, d_2\, {\kappa_2}^4 - 1.2\,10^3\, d_3\, {\kappa_2}^3 \\
&+ 39\, d_3\, {\kappa_2}^4 - 2.5\,10^3\, {d_1}^4 + 788\, {\kappa_2}^3 - 49\, {\kappa_2}^4 + {\kappa_2}^5 \\
&- 2.3\,10^3\, {d_1}^2\, {\kappa_2}^2 + 133\, {d_1}^2\, {\kappa_2}^3 + 300\, {d_1}^3\, {\kappa_2}^2 + 877\, {d_1}^2 d_2\, {\kappa_2}^2 \\
&- 2.2\,10^3\, {d_1}^2 d_3\, {\kappa_2}^2 + 80\, {d_1}^2 d_3\, {\kappa_2}^3 + 96\, {d_1}^3 d_3\, {\kappa_2}^2 \\
&+ 1.4\,10^5\, d_1 d_2\, \kappa_2 - 1\,10^4\, d_1 d_2\, {\kappa_2}^2 - 2.9\,10^4\, {d_1}^2 d_2\, \kappa_2 \\
&+ 244\, d_1 d_2\, {\kappa_2}^3 - 6.9\,10^3\, d_1 d_3\, {\kappa_2}^2 + 1.4\,10^4\, {d_1}^2 d_3\, \kappa_2 \\
&- 2.1\,10^4\, {d_1}^2 d_4\, \kappa_1 + 78\, d_1 d_3\, {\kappa_2}^3 - 1.9\,10^3\, {d_1}^3 d_3\, \kappa_2 \\
&+ 8\, d_1 d_3\, {\kappa_2}^4 - 3.5\,10^3\, d_4\, \kappa_1\, {\kappa_2}^2 + 177\, d_4\, \kappa_1\, {\kappa_2}^3 \\
&- 2\, d_4\, \kappa_1\, {\kappa_2}^4 + 1\,10^3\, d_1 d_4\, \kappa_1\, {\kappa_2}^2 + 3\,10^3\, {d_1}^2 d_4\, \kappa_1\, \kappa_2 \\
&- 24\, d_1 d_4\, \kappa_1\, {\kappa_2}^3 - 88\, {d_1}^2 d_4\, \kappa_1\, {\kappa_2}^2 - 1.4\,10^4\, d_1 d_4\, \kappa_1\, \kappa_2
\end{aligned} \tag{78}$$

$$\gamma_{14}(\kappa_1,\kappa_2) = {\kappa_2}^3 \left(4 d_1 + \kappa_2\right)^2 \left(64\, {d_1}^2 + 20\, d_1\, \kappa_2 + {\kappa_2}^2\right) \tag{79}$$

REFERENCES

[1] T. J. Roberts and E. Azizi, "Flexible mechanisms: the diverse roles of biological springs in vertebrate movement," *Journal of Experimental Biology*, vol. 214, no. 3, pp. 353–361, 2011.

[2] D. Rus and M. T. Tolley, "Design, fabrication and control of soft robots," *Nature*, vol. 521, no. 7553, p. 467, 2015.

[3] C. Laschi, M. Cianchetti, B. Mazzolai, L. Margheri, M. Follador, and P. Dario, "Soft robot arm inspired by the octopus," *Advanced Robotics*, vol. 26, no. 7, pp. 709–727, 2012.

[4] S. Seok, C. D. Onal, K.-J. Cho, R. J. Wood, D. Rus, and S. Kim, "Meshworm: a peristaltic soft robot with antagonistic nickel titanium coil actuators," *IEEE/ASME Transactions on mechatronics*, vol. 18, no. 5, pp. 1485–1497, 2013.

[5] H.-T. Lin, G. G. Leisk, and B. Trimmer, "Goqbot: a caterpillar-inspired soft-bodied rolling robot," *Bioinspiration & biomimetics*, vol. 6, no. 2, p. 026007, 2011.

[6] A. Albu-Schaeffer, O. Eiberger, M. Grebenstein, S. Haddadin, C. Ott, T. Wimboeck, S. Wolf, and G. Hirzinger, "Soft robotics," *IEEE Robotics & Automation Magazine*, vol. 15, no. 3, 2008.

[7] M. Hutter, M. Gehring, M. Bloesch, C. D. Remy, R. Y. Siegwart, and M. A. Hoepflinger, "Starleth: A compliant quadrupedal robot for fast, efficient, and versatile locomotion," 2012.

[8] M. Grebenstein, M. Chalon, W. Friedl, S. Haddadin, T. Wimböck, G. Hirzinger, and R. Siegwart, "The hand of the dlr hand arm system: Designed for interaction," *The International Journal of Robotics Research*, vol. 31, no. 13, pp. 1531–1555, 2012.

[9] F. Loeffl, A. Werner, D. Lakatos, J. Reinecke, S. Wolf, R. Burger, T. Gumpert, F. Schmidt, C. Ott, M. Grebenstein, *et al.*, "The dlr c-runner: Concept, design and experiments," in *Humanoid Robots (Humanoids), 2016 IEEE-RAS 16th International Conference on*, pp. 758–765, IEEE, 2016.

[10] M. Garabini, C. Della Santina, M. Bianchi, M. Catalano, G. Grioli, and A. Bicchi, "Soft robots that mimic the neuromusculoskeletal system," in *Converging Clinical and Engineering Research on Neurorehabilitation II*, pp. 259–263, Springer, 2017.

[11] C. Della Santina, C. Piazza, G. M. Gasparri, M. Bonilla, M. G. Catalano, G. Grioli, M. Garabini, and A. Bicchi, "The quest for natural machine motion: An open platform to fast-prototyping articulated soft robots," *IEEE Robotics & Automation Magazine*, vol. 24, no. 1, pp. 48–56, 2017.

[12] H. Hauser, A. J. Ijspeert, R. M. Füchslin, R. Pfeifer, and W. Maass, "Towards a theoretical foundation for morphological computation with compliant bodies," *Biological cybernetics*, vol. 105, no. 5-6, pp. 355–370, 2011.

[13] R. Pfeifer, M. Lungarella, and F. Iida, "The challenges ahead for bio-inspired'soft'robotics," *Communications of the ACM*, vol. 55, no. 11, pp. 76–87, 2012.

[14] A. Bicchi and G. Tonietti, "Fast and soft arm tactics," *Robotics & Automation Magazine, IEEE*, vol. 11, no. 2, pp. 22–33, 2004.

[15] S. Haddadin, M. Weis, S. Wolf, and A. Albu-Schäffer, "Optimal control for maximizing link velocity of robotic variable stiffness joints," *IFAC Proceedings Volumes*, vol. 44, no. 1, pp. 6863–6871, 2011.

[16] A. Velasco, G. M. Gasparri, M. Garabini, L. Malagia, P. Salaris, and A. Bicchi, "Soft-actuators in cyclic motion: Analytical optimization of stiffness and pre-load," in *Humanoid Robots (Humanoids), 2013 13th IEEE-RAS International Conference on*, pp. 354–361, IEEE, 2013.

[17] G. Buondonno and A. De Luca, "A recursive newton-euler algorithm for robots with elastic joints and its application to control," in *Intelligent Robots and Systems (IROS), 2015 IEEE/RSJ International Conference on*, pp. 5526–5532, IEEE, 2015.

[18] F. Petit, A. Daasch, and A. Albu-Schäffer, "Backstepping control of variable stiffness robots," *IEEE Transactions on Control Systems Technology*, vol. 23, no. 6, pp. 2195–2202, 2015.

[19] R. Lozano and B. Brogliato, "Adaptive control of robot manipulators with flexible joints," *IEEE Transactions on Automatic Control*, vol. 37, no. 2, pp. 174–181, 1992.

[20] C. Della Santina, M. Bianchi, G. Grioli, F. Angelini, M. G. Catalano, M. Garabini, and A. Bicchi, "Controlling soft robots: Balancing feedback and feedforward elements," *IEEE Robotics & Automation Magazine*, 2017.

[21] M. Hutter, C. D. Remy, M. A. Höpflinger, and R. Siegwart, "Slip running with an articulated robotic leg," in *Intelligent Robots and Systems (IROS), 2010 IEEE/RSJ International Conference on*, pp. 4934–4939, IEEE, 2010.

[22] D. Lakatos, G. Garofalo, F. Petit, C. Ott, and A. Albu-Schäffer, "Modal limit cycle control for variable stiffness actuated robots," in *Robotics and Automation (ICRA), 2013 IEEE International Conference on*, pp. 4934–4941, IEEE, 2013.

[23] G. Garofalo and C. Ott, "Energy based limit cycle control of elastically actuated robots," *IEEE Transactions on Automatic Control*, vol. 62, no. 5, pp. 2490–2497, 2017.

[24] R. J. Full and D. E. Koditschek, "Templates and anchors: neuromechanical hypotheses of legged locomotion on land," *Journal of Experimental Biology*, vol. 202, no. 23, pp. 3325–3332, 1999.

[25] N. Bernstein, "The co-ordination and regulation of movements," *The co-ordination and regulation of movements*, 1966.

[26] J. P. Scholz and G. Schöner, "The uncontrolled manifold concept: identifying control variables for a functional task," *Experimental brain research*, vol. 126, no. 3, pp. 289–306, 1999.

[27] J. P. Scholz and G. Schöner, "Use of the uncontrolled manifold (ucm) approach to understand motor variability, motor equivalence, and self-motion," in *Progress in Motor Control*, pp. 91–100, Springer, 2014.

[28] M. L. Latash, J. P. Scholz, and G. Schöner, "Motor control strategies revealed in the structure of motor variability," *Exercise and sport sciences reviews*, vol. 30, no. 1, pp. 26–31, 2002.

[29] Y. V. Mikhlin and K. V. Avramov, "Nonlinears normal modes for vibrating mechanical systems. review of theoretical developments," *Applied Mechanics Reviews*, vol. 63, no. 6, p. 060802, 2010.

[30] D. Lakatos, W. Friedl, and A. Albu-Schäffer, "Eigenmodes of nonlinear dynamics: Definition, existence, and embodiment into legged robots with elastic elements," *IEEE Robotics and Automation Letters*, vol. 2, no. 2, pp. 1062–1069, 2017.

[31] S. Grazioso, V. Sonneville, G. Di Gironimo, O. Bauchau, and B. Siciliano, "A nonlinear finite element formalism for modelling flexible and soft manipulators," in *Simulation, Modeling, and Programming for Autonomous Robots (SIMPAR), IEEE International Conference on*, pp. 185–190, IEEE, 2016.

[32] F. Renda, F. Boyer, J. Dias, and L. Seneviratne, "Discrete cosserat approach for multi-section soft robots dynamics," *arXiv preprint arXiv:1702.03660*, 2017.

[33] S. H. Sadati, S. E. Naghibi, I. D. Walker, K. Althoefer, and T. Nanayakkara, "Control space reduction and real-time accurate modeling of continuum manipulators using ritz and ritz–galerkin methods," *IEEE Robotics and Automation Letters*, vol. 3, no. 1, pp. 328–335, 2018.

[34] C. Della Santina, R. K. Katzschmann, A. Bicchi, and D. Rus, "Dynamic control of soft robots interacting with the environment," *1st IEEE Soft Robotics Conference*, 2018.

[35] F. Renda and L. Seneviratne, "A geometric and unified approach for modeling soft-rigid multi-body systems with lumped and distributed degrees of freedom," in *Robotics and Automation (ICRA), 2018 IEEE International Conference on*, IEEE, 2018.

[36] M. Dahleh, M. A. Dahleh, and G. Verghese, "Lectures on dynamic systems and control," *A+ A*, vol. 4, no. 100, pp. 1–100, 2004.

[37] J. Henrard, "Lyapunov's center theorem for resonant equilibrium," *Journal of Differential Equations*, vol. 14, no. 3, pp. 431–441, 1973.

[38] R. Rosenberg, "On nonlinear vibrations of systems with many degrees of freedom," *Advances in applied mechanics*, vol. 9, pp. 155–242, 1966.

[39] T. Caughey, A. Vakakis, and J. Sivo, "Analytical study of similar normal modes and their bifurcations in a class of strongly non-linear systems," *International Journal of Non-Linear Mechanics*, vol. 25, no. 5, pp. 521–533, 1990.

[40] A. Nayfeh, C. Chin, and S. Nayfeh, "On nonlinear normal modes of systems with internal resonance," *TRANSACTIONS-AMERICAN SOCIETY OF MECHANICAL ENGINEERS JOURNAL OF VIBRATION AND ACOUSTICS*, vol. 118, pp. 340–345, 1996.

[41] A. F. Vakakis, L. I. Manevitch, Y. V. Mikhlin, V. N. Pilipchuk, and A. A. Zevin, *Normal modes and localization in nonlinear systems*. Springer, 2001.

[42] R. Rand, C. Pak, and A. Vakakis, "Bifurcation of nonlinear normal modes in a class of two degree of freedom systems," *Acta Mech*, vol. 3, no. 1, pp. 129–45, 1992.

[43] S. W. Shaw and C. Pierre, "Normal modes for non-linear vibratory systems," *Journal of sound and vibration*, vol. 164, no. 1, pp. 85–124, 1993.

[44] S. Kobayashi and K. Nomizu, *Foundations of differential geometry*, vol. 2. Interscience publishers New York, 1969.

[45] B. Finlayson and L. Scriven, "The method of weighted residualsa review," *Appl. Mech. Rev*, vol. 19, no. 9, pp. 735–748, 1966.

[46] G. I. Cirillo, A. Mauroy, L. Renson, G. Kerschen, and R. Sepulchre, "A spectral characterization of nonlinear normal modes," *Journal of Sound and Vibration*, vol. 377, pp. 284–301, 2016.

[47] E. Pesheck, C. Pierre, and S. Shaw, "A new galerkin-based approach for accurate non-linear normal modes through invariant manifolds," *Journal of sound and vibration*, vol. 249, no. 5, pp. 971–993, 2002.

[48] L. Renson, G. Kerschen, and B. Cochelin, "Numerical computation of nonlinear normal modes in mechanical engineering," *Journal of Sound and Vibration*, vol. 364, pp. 177–206, 2016.

[49] K. V. Avramov and Y. V. Mikhlin, "Review of applications of nonlinear normal modes for vibrating mechanical systems," *Applied Mechanics Reviews*, vol. 65, no. 2, p. 020801, 2013.

[50] B. Siciliano and O. Khatib, *Springer handbook of robotics*. Springer, 2016.

[51] R. A. Horn and C. R. Johnson, *Matrix analysis*. Cambridge university press, 2012.

[52] D. Lakatos, M. Görner, F. Petit, A. Dietrich, and A. Albu-Schäffer, "A modally adaptive control for multi-contact cyclic motions in compliantly actuated robotic systems," in *Intelligent Robots and Systems (IROS), 2013 IEEE/RSJ International Conference on*, pp. 5388–5395, IEEE, 2013.

[53] R. Goebel, R. G. Sanfelice, and A. R. Teel, "Hybrid dynamical systems," *IEEE Control Systems*, vol. 29, no. 2, pp. 28–93, 2009.

[54] H. Geyer, A. Seyfarth, and R. Blickhan, "Compliant leg behaviour explains basic dynamics of walking and running," *Proceedings of the Royal Society of London B: Biological Sciences*, vol. 273, no. 1603, pp. 2861–2867, 2006.

[55] G. Garofalo, C. Ott, and A. Albu-Schäffer, "Walking control of fully actuated robots based on the bipedal slip model," in *Robotics and Automation (ICRA), 2012 IEEE International Conference on*, pp. 1456–1463, IEEE, 2012.

[56] K. B. Petersen, M. S. Pedersen, *et al.*, "The matrix cookbook," *Technical University of Denmark*, vol. 7, p. 15, 2008.

[57] H. Rosenbrook, "The stability of linear time-dependent control systems," *INTERNATIONAL JOURNAL OF ELECTRONICS*, vol. 15, no. 1, pp. 73–80, 1963.

[58] L. H. Duc, A. Ilchmann, S. Siegmund, and P. Taraba, "On stability of linear time-varying second-order differential equations," *Quarterly of applied mathematics*, vol. 64, no. 1, pp. 137–152, 2006.